ELSEVIER

Biophysical Chemistry 134 (2008) 119–143

Biophysical Chemistry

http://www.elsevier.com/locate/biophyschem

Ion homeostasis and the functional roles of SERCA reactions in stimulus–secretion coupling of the pancreatic β-cell A mathematical simulation

Frank Diederichs

Marschweg 10, D-29690 Schwarmstedt, Germany

Received 22 December 2007; received in revised form 20 January 2008; accepted 4 February 2008
Available online 15 February 2008

Abstract

The present paper concerns with ion homeostatic reactions in view of stimulus–secretion coupling of the β-cell, including Ca^{2+} fluxes of the endoplasmatic reticulum (ER). A steady state of cytosolic sodium and potassium ion concentrations ($[Na^+]_c$ and $[K^+]_c$, respectively), and of the membrane potential ($\Delta_c\phi$) can be attained only, if the flux through the electrogenic Na-K pump (J_{NaK}) is balanced electrically, and if J_{NaK} is rather high (about 25% of total ATP consumption at 10 mM glucose). Metabolically caused changes of cellular pH are unlikely, because, on the one hand, CO_2 can rapidly leave the cell through cellular membranes, and because ATP cycling cannot produce nor consume protons. A slight decrease of pH_c during cellular activity is caused mainly by an increased Ca-H exchange flux through the plasma membrane Ca^{2+} pump (J_{PMCA}), which might be overcome, however, by H^+ transport into secretory granules. The present simulations show that the conductance of ATP-sensitive K^+ channels (K_{ATP}) is highly susceptible to changes of $[Mg^{2+}]_c$. As a physical link between the Ca^{2+} filling state of the ER and the initiation of a depolarising, Ca^{2+} release-activated current (I_{CRAN}), a metabolite (inositol 1,4,-diphosphate (IP_2)) of the inositol 1,4,5-triphosphate (IP_3) cycle is introduced. Sufficient ATP for insulin secretion is made available during glucose activation by $[IP_2]$ inhibition of a parallel $[ATP]_c$ consuming flux through protein biosynthesis (J_{Pbs}). This leads to fast oscillations with a triphasic patterns of $[Ca^{2+}]_c$ oscillations. Slow oscillations are initiated by including a Ca^{2+} leak current through highly uncoupled SERCA3 pumps. Both types of oscillations may superimpose yielding compound bursting and mixed oscillations of $[Ca^{2+}]_c$.

Keywords: Cell pH; Na-K pump; Membrane potential; Ca^{2+} oscillations; SERCA uncoupling; Stimulus–secretion coupling

1. Introduction

Many important results of pancreatic β-cell research were derived from electrophysiological approaches, especially from measurements of $\Delta_c\phi$ and $[Ca^{2+}]_c$. In β-cells amazingly little is known about other parameters of biophysical interest such as $[Na^+]_c$, potassium $[K^+]_c$, $[Mg^{2+}]_c$, and hydrogen ion activity ($[H^+]_c$). From biochemical thermodynamics it is known that both, pH and pMg can strongly influence concentrations of ATP, ADP, and Pi species, and thus, cytosolic and mitochondrial standard transformed Gibbs energies of reaction ($\Delta_rG'^{o}$ (ATP_c) and $\Delta_rG'^{o}$ (ATP_m), respectively [1]). Furthermore, those transport processes, in which these species are involved, may also be affected. These processes are ATP^{4-}/ADP^{3-} exchange by the adenine nucleotide translocator (J_{AE}) and $H^+/H_2PO_4^-$ symport by the phosphate carrier (J_{Pi}), both at the inner mitochondrial membrane.

Because K_{ATP} channels are known to be controlled in β-cells by ATP and ADP species [2], insulin secretion might be influenced also thermodynamically by $[H^+]$ and/or $[Mg^{2+}]$-dependent species formation.

The electrogenic Na-K pump controls cellular ion homeostasis [3–5]. It does not only adjust $[Na^+]_c$ and $[K^+]_c$, but is also responsible for the generation and control of $\Delta_c\phi$. The resting $\Delta_c\phi$ is usually calculated using constant concentrations of extra- and intracellular ions. The pump flux of the Na-K pump is usually not considered. The assumption of non-changing ion concentrations, however, is reliable only during a short time interval. Because without pumping, $[K^+]_c$ would continuously decrease, $[Na^+]_c$ increase, and $\Delta_c\phi$ would become depolarised. Therefore, for a more realistic description of

E-mail address: fwkh.diederichs@web.de.

0301-4622/$ - see front matter © 2008 Elsevier B.V. All rights reserved.
doi:10.1016/j.bpc.2008.02.001

cellular ion homeostasis and of $\Delta_c\phi$, besides $\Delta_c\phi$, additionally $[Na^+]_c$ and $[K^+]_c$ must be taken into account in calculations as time-dependent variables.

Concerning stimulus secretion coupling of the pancreatic β-cell the question arises, to which degree a hyperpolarising Na-K pump current (I_{NaK}) may interfere with glucose-induced activation of metabolism and the mandatory depolarisation of $\Delta_c\phi$. In addition, the pump may abolish the inactivation of K_{ATP} channels by an additional $[ADP]_c$ production, which likewise could prevent depolarisation.

In this context, another problem has to be answered, namely how the β-cell's power output machinery can deliver sufficient ATP_c to satisfy the demands of increased ATP_c consumption during activation. In the β-cell, the metabolic flux through glycolysis (GLY) and citric acid cycle (CAC) is limited by the activity of the recognition enzyme glucokinase (GK). A strong activation as in skeletal muscle cells cannot be expected, because moreover the β-cell does also not have any noteworthy depot of metabolic fuel like for instance glycogen, which could be recruited for a markedly increased ATP demand.

It could be demonstrated experimentally [6–8] that islet β-cells respond to an activating glucose concentration with a first decrease of $[Ca^{2+}]_c$ below steady state values (phase 0), which is followed by a pronounced and prolonged increase of $[Ca^{2+}]_c$ (phase 1) [9], and thereafter with a switch over into oscillations of $[Ca^{2+}]_c$ (phase 2). It is widely accepted that phases 1 and 2 are produced by changes of $\Delta_c\phi$. Phase 1 is kinetically coupled to a period of continuous spiking of $\Delta_c\phi$ and phase 2 to $\Delta_c\phi$ oscillations, whereas phase 0 seems to be brought about mainly by Ca^{2+} pumping of the sarco/endoplasmatic reticulum Ca^{2+}ATPase (SERCA) [10]. It was assumed that the luminal Ca^{2+} concentration of the ER ($[Ca^{2+}]_{lu}$) is functionally involved with phase 1. In fact, it was observed that the filling state of this organelle may be linked to opening of non-selective cation channels of the cell membrane, which by depolarisation may extend bursting of $\Delta_c\phi$ during phase 1 [8,9]. The nature of this link, however, is not known so far.

R. Bertram and colleagues [11–13] hypothesised that the glycolytic enzyme phosphofructo kinase (PFK) may generate slow oscillations, on which fast, "electrical" oscillations may be superimposed, so that so-called compound oscillations may result. Beauvois et al. [14] could show that the behaviour of SERCA pumps may be crucially involved with the generation of slow oscillations of $[Ca^{2+}]_c$ and $\Delta_c\phi$. She suggested that "mixed" $[Ca^{2+}]_c$ oscillations are produced by an interaction of fast oscillations with slow ones and showed that the isoform SERCA3 is a necessary prerequisite for the generation of mixed oscillation.

It was the aim of this study to show how pH- and pMg-dependent changes on $[ADP]_c$ and $[ATP]_c$ species formation may interfere with cellular energetics and in particular with the behaviour of K_{ATP} channels. Ion homeostatic reactions of the β-cell are included in simulations to see if stimulus-secretion coupling is compatible with these reactions, especially with a high power output of the Na-K pump. In addition it ought to be shown, how the triphasic dynamics of $[Ca^{2+}]_c$ may be accomplished. The results will show that the involvement of ER reactions can reproduce patterns of fast and slow oscillations, including compound bursting [15,16] and mixed $[Ca^{2+}]_c$ oscillations [14].

2. Methods

In a previous publication a novel formalism was introduced, which describes by phenomenological equations membrane as well as metabolic fluxes [17]. This formalism is being used consecutively also in this paper.

For a more realistic description of cellular reactions the cytosolic volume V_c is reduced to 72% of the cell volume, V_{cell}. This changes the conversion factor α_c from 9.4843 to 12.5135×10^{12} μM/C. Thus, to yield the cytosolic flux J in μM/ms, the membrane current has to be multiplied by this factor: $J\,(\mu M/ms)=12.5135\times10^{12}\times I\times10^{-18}$ (μM/C × C/ms) (C = Coulomb, I = numerical value of current I) or $J=12.5135\times10^{-6}\times I$. From $\alpha_m=180.194\times10^{12}$ μM/C, $\alpha_m/\alpha_c=V_c/V_m=Q_V=14.4$ can be obtained.

In addition to the cytosol and the mitochondrial matrix a third compartment is introduced, the ER, with $V_{ER}=0.05\times V_{cell}$, and $\alpha_r=\alpha_m$.

All biochemical equilibrium constants (K's) were taken from Alberty [1]. The equilibrium constant for ATP hydrolysis is now given as a function of pH and pMg (see Appendix, A1–A10).

$[Mg^{2+}]_c$ and $[Mg^{2+}]_m$ are set constant to 0.8 mM. In biochemistry and physiology the measure of proton concentration usually is related to pH, that is, to proton activity. All respective constants of Alberty, however, are related to proton concentration at given ionic strength and temperature. Therefore, these constants had to be transformed into so-called mixed constants by transforming proton concentration into proton activity at 0.25 M ionic strength and 310 K and taking 1.0 μM as unit activity. For instance, the following $\Delta_rG'^{o}(ATP)$ values for normal pH_c and pH_m are calculated: for cytosolic ATP hydrolysis at $pH_c=7.2$, 0.8 mM Mg^{2+}, 0.25 M ionic strength, 310 K, and $K^{ref1}=6.2666\times10^5$, $\Delta_rG'^{o}(ATP_c)=34.204$, and under the same conditions of the mitochondrial matrix but $pH_m=7.5$, $\Delta_rG'^{o}(ATP_m)=35.535$ kJ/mol.

Equilibrium constants of metabolic reactions are given for 0.25 M ionic strength, 298 K, and fixed pH values of $pH_c=7.2$ and $pH_m=7.5$, although these constants may change appreciably with pH and/or temperature. However, a rather large change of these constants modifies numerical results of flux calculations only slightly, and, moreover, may be compensated by adjusting the respective maximal conductance.

Calculations were performed using Mathcad® 2001*i* Professional, including Solving & Optimisation Extension Pack. The program's solver *Radau* was used to solve numerically a given set of differential equations. Calculations were run on a desktop Intel(R) Core(TM) 2CPU @ 2.00 GHz 1.99 GB RAM under Microsoft® Windows XP PRO.

3. Results and discussion

For treatment of cellular ion homeostasis, proton activity $[H^+]_c$ ($[H^+]_m$ was already considered), $[Na^+]_c$ and $[K^+]_c$, $[HCO_3^-]_m$ and $[HCO_3^-]_c$, and $[CO_2]_m$ and $[CO_2]_c$ are included as variables. As already mentioned in the methods section, $[Ca^{2+}]_{lu}$ of the ER is now also included as a further variable.

As will be treated in detail below, $[Ca^{2+}]_{lu}$ interacts indirectly with a special channel of the cell membrane to activate a depolarising, non-selective cation current (I_{CRAN}, for flux equation and parameters

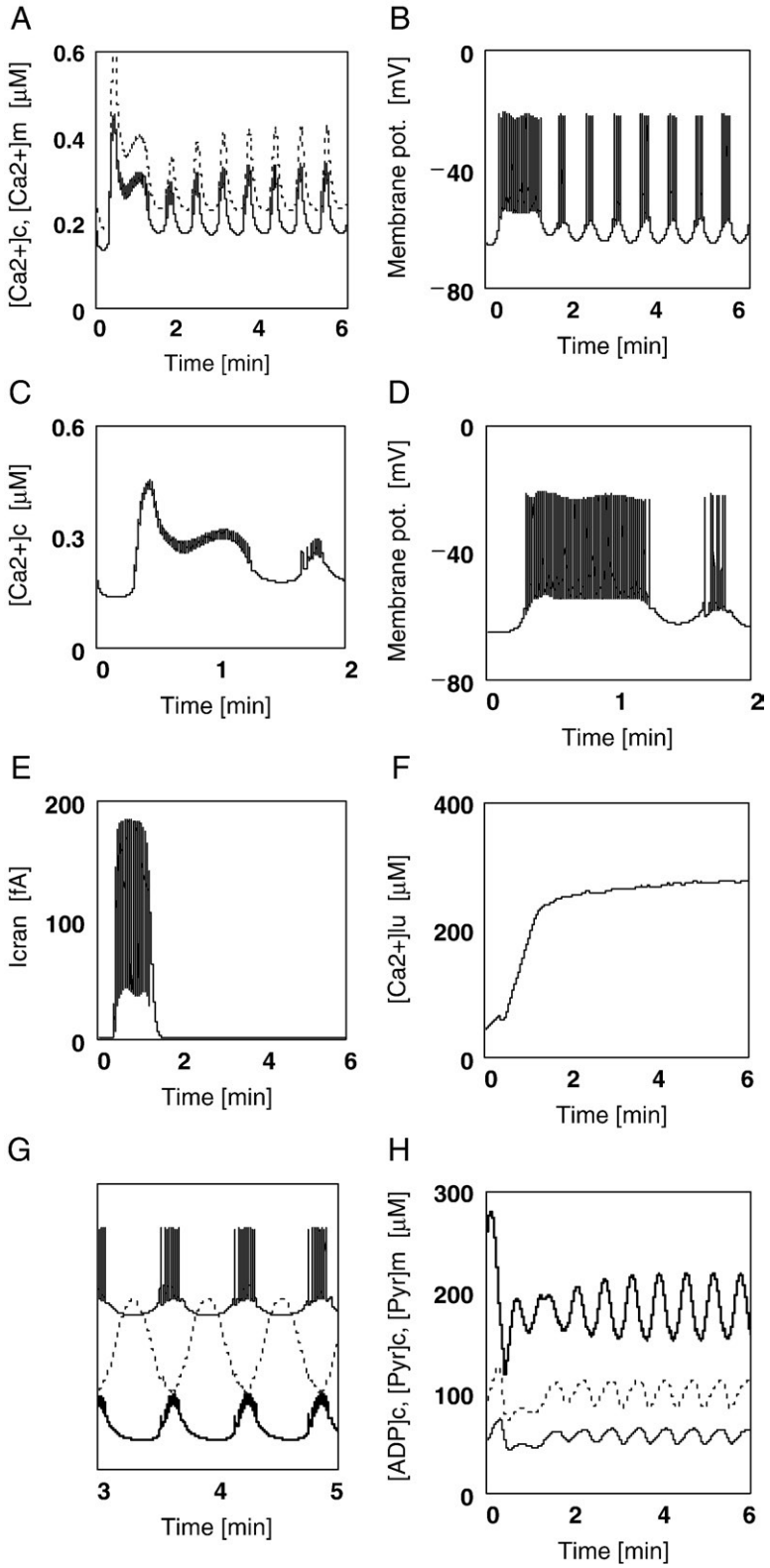

Fig. 1. Fast (K_{ATP}) oscillations at 10 mM [Glu]. (A) (line) $[Ca^{2+}]_c$; (dot) $[Ca^{2+}]_m$. (B) (line) $\Delta_c\phi$ (C) (line) $[Ca^{2+}]_c$ phases during first 2 min. (D) (line) $\Delta_c\phi$ during first 2 min. (E) (line) transient I_{CRAN}. (F) (line) $[Ca^{2+}]_{lu}$. (G) (line) $\Delta_c\phi$; (dot) G_{Katp}; (bold line) $[Ca^{2+}]_c$, ordinates of $\Delta_c\phi$ and $[Ca^{2+}]_c$ are transformed to be comparable with G_{Katp}. (H) (bold line) $[ADP]_c$; (dot) $[Pyr]_m$; (line) $[Pyr]_c$.

see Appendix A38a–d). It is hypothesised that this interaction may proceed via an IP_3 metabolite produced in dependency on the Ca^{2+} filling state of the ER. M. J. Berridge [18] could show that after a certain stimulus PIP_2 of the cell membrane becomes hydrolysed to produce diacylglycerol (DAG) and IP_3. This latter compound is consecutively dephosphorylated to inositol (In)

forming IP_2 and inositol 1,-phosphate (IP) as intermediates. Inositol is further processed via phosphatidylinositol and coupled ATP consumption to produce PIP_2 again.

To model this cyclic reaction sequence it was necessary to include [PIP_2], [DAG], [IP_3], [IP_2], and [In] as variables in simulations (A25–28).

It is hypothesised further that in addition to $[Ca^{2+}]_c$, [DAG] may be involved in the activation of insulin secretion. These rather complex interactions between IP_3 cycle, ER reactions, and activation of exocytotic insulin release will be handled in more detail below.

3.1. Biochemical constraints of glucose oxidation

It seems noteworthy to emphasise that the present simulations, despite the large number of variables, do fulfil the constraints of oxidative glucose metabolism, that is, at steady state, in a given time interval 6 mol of CO_2 are formed and 6 mol of O_2 are consumed per mole of metabolised glucose. At 4 mM [Glu] $J_{O2}^{tam}/J_{GK}^{tam}=6$ (B1, B10, tam=time averaged mean). Under conditions of glucose activation (Figs. 1 and 2) this quotient approaches 6.0 (4.5–10 during oscillations). In addition, for the production of reduced nicotinamid dinucleotide and flavin mononucleotide (NAD_{red} and FAD_{red}, respectively) simulations must yield the biochemical stoichiometry of 12 reducing equivalents per mole glucose. At steady state this value is 12, and approaches 12 (8.7–20) during oscillations. The respiratory quotient (RQ) value equals 1.0 under all conditions.

In a similar way, cytosolic ATP production may be used to compare the output of simulations with the requirements of biochemistry. This value, however, depends on the degree of coupling of oxidative phosphorylation (uncoupling is here solely produced by a leak flux of protons (J_{PL}, B13) from the intra membrane space into the mitochondrial matrix) and on the extent of Ca^{2+} cycling (via Ca^{2+} uniport (J_{CU}, B11) and H/Ca exchange (J_{HCE}, B12)) over the inner mitochondrial membrane. With given stoichiometries of 10 H^+ per NAD_{red} oxidised and 6.0 H^+ per FAD_{red} oxidised, 3.0 H^+ per ATP_m and 4.0 H^+ per ATP_c formed (B8, B9, A11), the theoretical value (no uncoupling and no Ca^{2+} cycling) lies between 29.5 and 31 mol ATP_c per mole glucose, depending on the ratio of glycolytical FAD_{red} to total glycolytically produced reducing equivalents. At 4.0 mM [Glu] this value is 30.69 mol ATP_c per mole of metabolised glucose. When J_{PL} and $2.0\times J_{CU}$ were non-zero, as observed under physiological conditions [19] and conditions of simulations presented here, a value of 27.23 is reached.

3.2. $[Na^+]_c$, $[K^+]_c$, the Na-K pump, and $\Delta_c\phi$

The Na-K pump in the present simulations produces a relatively strong outward current of more than 30% (of total outward current), and an associated large ATP consumption of about 31% and 25% at 4.0 and 10.0 mM [Glu], respectively (total ATP consumption (J_P, A36) increases during activation by about 51.0%). To avoid interferences with the mechanisms of stimulus-secretion coupling, the electrical and energetic effects of these fluxes should be compensated. This is achieved by introducing a depolarising Na^+ leak current (A39, $I_{Lna}=1.94$ pA under resting conditions). Together with the Ca^{2+} current (B15, $I_{Cav}=1.63$ pA under resting conditions) through Ca_V channels both currents counteract the hyperpolarising I_{NaK} (J_{NaK}/α_c, A32) adequately, to yield a stable steady state $\Delta_c\phi$ under resting conditions. From experimental results of Göpel et al. [20] it can be taken that total Na^+ and total Ca^{2+} currents are both markedly more pronounced under resting conditions. It seems justified therefore to include, in addition to I_{Cav}, a Na^+ leak current to sufficiently counteract I_{NaK}.

However, not only charges have to be balanced over the cell membrane, but also concomitant pump fluxes of Na^+ and K^+ should be allowed to reach a steady state. This means that the basic cellular K^+ conductance (G_{Katp}^{max}, A40) has to be adjusted appropriately to yield reliable steady state values also of $[Na^+]_c$ and $[K^+]_c$. The outward pump flux of Na^+ has to be matched not only by the leak inward flux, but in addition by an electroneutral Na^+ influx via Na/H exchange (J_{NHE}, A21). In real β-cells, additional Na^+-coupled transport reactions may exist such as amino acid or Na-HCO_3 cotransport, which, however, are not considered here. Beside the pump flux also these Na^+ inward fluxes are involved with the adjustment of $[Na^+]_c$ and consequently with the tuning of $[Na^+]_c$-activated J_{NaK}. Na^+ influx via Na/Ca exchange (J_{NCE}, B14) at rather low $[Ca^{2+}]_c$ is of minor importance.

During glucose activation, $[K^+]_c$ decreases slightly (Fig. 2C). This is caused mainly by a depolarised $\Delta_c\phi$, that is, by an increased driving force for K^+ efflux via K_{ATP} (A40) and K^+ delayed-rectifier (K_{Re}, B16) channels. $[Na^+]_c$ increases slightly under these conditions, mainly because J_{NHE} becomes activated by acidification.

3.3. ATP cycling and pH

Gibbs free energy of cellular glucose oxidation is coupled to ATP formation, which occurs mainly by oxidative phosphorylation in mitochondria and to a minor part by GLY. This ATP is entirely consumed by cytosolic work generating reactions like insulin secretion, ion pumps, and cellular protein biosynthesis. That is, ATP has to pass cyclically through producing and consuming reactions. This behaviour of energy metabolism imposes, however, a serious constraint on this ATP cycle: the line integral (LI) over the closed path of all potential differences of ATP must vanish. This integral is given by the sum of all driving forces A ($A=-\Delta_rG$), which are passed through during ATP formation in mitochondria, transport of ATP into the cytosol, ATP splitting in the cytosol, and transport of splitted ATP back into mitochondria (A11–13, A19, 20). The results show that LI=0 is verified for all simulations tested, as well at steady state as during oscillations.

From this behaviour an important conclusion about pH shifts in the cytosol and in the mitochondrial matrix can be drawn: if ATP production and consumption proceed in a closed cycle as it is suggested for the living cell under physiological conditions, there cannot be neither acid production nor consumption. This is valid for the cytosol equally like the mitochondrial matrix.

In the present simulations glucose oxidation is related to $[CO_2]$ and not to total CO_2 concentration, which contains all

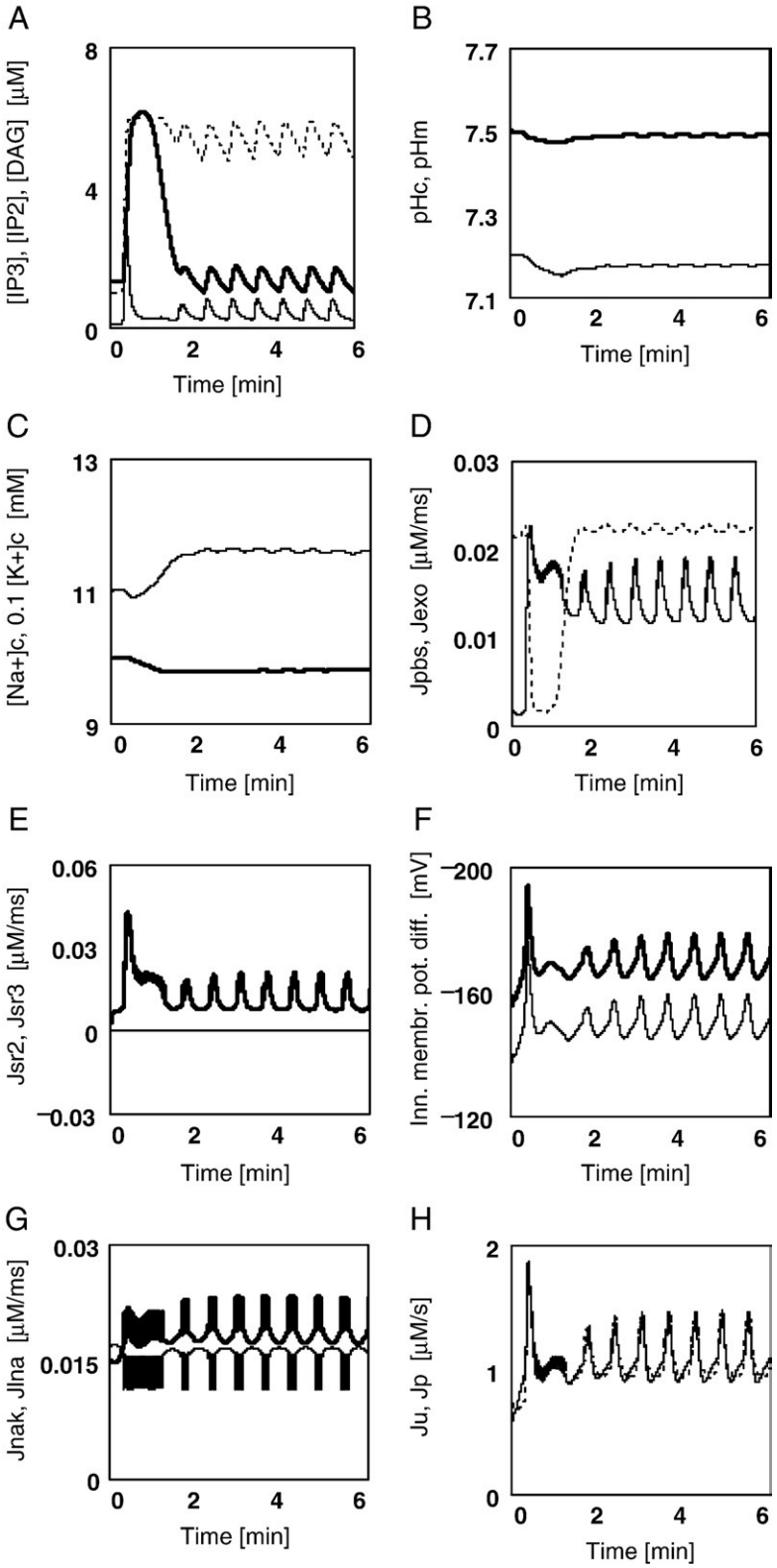

Fig. 2. Fast (K_{ATP}) oscillations at 10 mM [Glu]. (A) (dot) DAG; (bold line) IP_2; (line) IP_3. (B) (bold line) pH_m; (line) pH_c. (C) (line) $[Na^+]_c$; (bold line) $[K^+]_c$. (D) (dot) J_{Pbs}; (line) J_{Exo}. (E) (bold line) J_{SR2}; (line) $J_{SR3}=0$. (F) (bold line) $\Delta\,\tilde{\mu}_H$; (line) $\Delta_m\phi$. (G) (bold line) J_{NaK}; (line) J_{Lna}. (H) (line) J_U; (dot) J_P.

species of this compound. Thus, there is no proton production by this reaction up to CO_2 formation. Because CO_2 permeability of membranes may be appreciably higher than CO_2 flux through the carbonic anhydrase reaction (J_{CA}, A18a, A18b), the metabolically formed CO_2 may leave the cell practically without intracellular proton production.

During glucose metabolism most reducing equivalents are produced in the mitochondrial matrix and are reoxidised by

respiratory chain reactions (J_{NA} and J_{FA}, B8, B9), so that also these reactions cannot change pH_m. Cytosolic reducing equivalents are in part directly (glycerophosphate shuttle, J_{GS}, B6) or indirectly shuttled (malate–aspartate shuttle, J_{MS}, B7a,b) between cytosol and mitochondria. J_{MS} consumes one "electrochemical" proton, which, however, is recycled by respiratory chain fluxes (J_{NA} and J_{FA}, B8, 9). J_{Pi} plus J_{AE} (A12, 13) are together coupled to one "electrochemical proton", which is in the same manner recycled. During GLY, practically two protons are produced. They are needed for pyruvate cotransport (B5) into the mitochondrion, where they finally are consumed by the pyruvate dehydrogenase reaction (J_{PDH}, (A23).

Summing up, glucose metabolism in accordance with textbook biochemistry (without lactate production) can neither produce nor consume protons as long as coupled cycles were not disrupted, and glycolytical pyruvate production and pyruvate consumption by mitochondria remained continuous.

Alberty [1, Table 4.12] determined a value of 12.4 for the change of proton binding by reactions of GLY plus PDH plus CAC (here B1–4, A23, 24). However, in these calculations reoxidation of reducing equivalents and consumption of ATP were not included. Furthermore, reactions were related to the sum of CO_2 species. Therefore, a zero change of proton binding, as it is suggested here, cannot be in accordance with the above results of Alberty.

3.4. Buffering and intracellular acidification during activation

The changes of intracellular pH depend on the buffering power β of respective compartments. Here, it is assumed that the intrinsic mitochondrial and cytosolic buffering powers (β_m^{Bu} and β_c^{Bu}, respectively, A16) are equal (pH and buffering power of ER is not included in simulations). According to [21] β^{Bu} is defined as total buffering power minus that of the CO_2/HCO_3^- system (A18a, b). At 4.0 mM [Glu] total mitochondrial and cytosolic buffering powers amount to about $\beta_m^{tot}=75$ and $\beta_c^{tot}=60$ mM, respectively. The values for β_m^{CO2} and β_c^{CO2} are 69 and 35 mM, respectively. At 10 mM [Glu] respective values are all slightly reduced through an also only negligible decreased pH (Fig. 2B).

Buffering reactions like that of J_{CA} (A18a, b) may proceed in the direction of proton production or consumption, or may be at equilibrium, depending on the value of the respective driving force (positive, negative, or zero). This means that not only pH shifts into both directions can be computed, but also oscillations of a certain reaction X around equilibrium, that is around $A_x=0$, should be possible, presupposed these oscillations are forced by other driving forces than A_x. The description of such reactions is possible only if a driving force is included in the flux equation [cf. 17].

From Fig. 2B it can be taken that pH_m and pH_c both fall slightly from steady state values of 7.5 and 7.2 at [Glu]= 4.0 mM to values of about 7.487 and 7.175, respectively, during activation by 10 mM [Glu]. These changes of pH values could not have been brought about by glucose metabolism or the ATP cycle as is shown above, but must have been produced by other proton generating reactions. These are given by J_{PMCA} (A33) and fluxes through Ca^{2+} pumps of the ER membrane (SERCA2 and SERCA3, J_{SR2} and J_{SR3}, respectively (A29, 30)). Mainly J_{PMCA} and J_{SR2} contribute to an acidification of the cytosol. The mitochondrial matrix, on the other hand, becomes acidified due to a net influx of "electrochemical" protons. The net proton current over the inner membrane, however, is outward directed (negative), so that $\Delta_m\phi$ becomes hyperpolarised. Therefore, the matrix must have been acidified by J_{Pi} (A12), which is slightly more pronounced than J_{AE} (A13) during the first second.

The pH_c decrease is counteracted by proton efflux via J_{NHE} (A21) of the cell membrane. This reaction increases during activation (not shown). Like in other cell types also in the pancreatic β-cell additional pH_c regulatory mechanisms may exist (as for instance Na-HCO_3 cotransport), which, however, are not considered in the present simulations.

Insulin release from β-cells is accomplished by exocytosis of insulin containing granules. A vacuolar-type ATP-dependent H^+ pump in conjunction with a Cl^- channel acidifies granules. The low granular pH may "prime" granules for Ca^{2+}-dependent exocytosis [22]. Stiernet et al. could demonstrate that glucose activation decreases granular pH, while pH_c increases [23]. Doliba et al. [24] measured also a slowly increasing pH at high [Glu]. The results of present simulations are not in accordance with these experimental results. Presumably the increase of pH_c is primarily caused by H^+ pumping of the granular H^+ pump, which overcomes the Ca^{2+}-dependent acidification by J_{PMCA} and J_{SR2}. Because the underlying mechanisms of priming and exocytosis are not exactly known, these reactions of granular H^+ transport were not considered here. This might explain why the present results of pH_c are not in accordance with recent findings of pH measurements in β-cells.

3.5. $[Mg^{2+}]_c$ and K_{ATP} channel behaviour

The K_{ATP} channel opening probability (OP) is highly susceptible to changes of $[Mg^{2+}]_c$. This dependency is brought about by participating species $[MgADP^-]_c$, $[ATP^{4-}]_c$, and $[ADP^{3-}]_c$ (this model), which change appreciably, when respective polynomials are altered by $[Mg^{2+}]_c$ (Fig. 3). This behaviour strongly requests a powerful control of $[Mg^{2+}]_c$ to

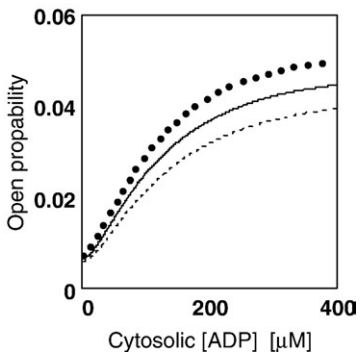

Fig. 3. Influence of $[Mg^{2+}]_c$ on open probability of K_{ATP} channels at $pH_c=7.2$. (bold dot) $[Mg^{2+}]_c=0.9$ mM; (line) $[Mg^{2+}]_c=0.8$ mM, this concentration is used as a constant parameter in all simulations; (dot) $[Mg^{2+}]_c=0.7$ mM.

avoid an uncontrolled influence of this ion on K_{ATP} channel activity (A40).

Henquin and Lambert [25] could show that insulin release from islets is severely reduced in HEPES buffered media compared to HCO_3^- containing media. Carroll et al. [26] demonstrated that inactivation of K_{ATP} channels was abolished under such conditions. This latter effect cannot be explained by a passively altered $[Mg^{2+}]_c$ brought about by a transiently increased pH_c under such conditions (HCO_3/CO_2 withdrawal), because $[Mg^{2+}]_c$ presumably would be decreased by increased binding, and thus would close K_{ATP} channels. If it is assumed, however, that the high susceptibility for $[Mg^{2+}]_c$ were damped by a pH_c-dependent control site of the channel, then the behaviour could be explained. In fact, a decrease of $[Mg^{2+}]_c$ through an elevated pH_c and associated K_{ATP} inactivation would be counteracted by an increase of the channels OP at increased pH_c, and vice versa. At lowered pH_c during glucose activation it would overcome a possible drop of $[Mg^{2+}]_c$. These possibilities were, however, not considered in simulations, because until the present time too little is known about cellular transport and binding of this cation.

MacGregor et al. [27] could show that PIP_2 and other phospholipids antagonise ATP inhibition of K_{ATP} channels. Because PIP_2 concentration is high at sub-stimulatory and rapidly decreased at stimulatory [Glu], also this mechanism would be helpful to protect β-cells against an unwanted initiation of insulin release by a drop of $[Mg^{2+}]_c$.

3.6. Energetic requirements of β-cell activation

It is currently widely accepted that activation of pancreatic β-cells is initiated metabolically by an increase of blood glucose concentration (in simulations from 4 to 10 mM). Unlike the activation process of a skeletal muscle cell, the β-cell first has to decrease $[ADP]_c$, which is followed by an increase of $[Ca^{2+}]_c$ and (this model, [cf. 17]) only thereafter by a further $[Ca^{2+}]_m$-dependent activation of mitochondrial ATP production. The flux through entire glucose oxidation and coupled ATP production depends strongly on GK activity. Therefore, ATP production as well as ATP consumption must be limited by J_{GK} (B1). This flux increases from 1.81 μM/ms at 4 mM to 2.71 μM/ms at 10 mM [Glu] (relative increase amounts to about 50%, Table 1). ATP consumption is increased by 47.5 and 41.8%, respectively (cells containing SERCA3 (see below) show a slightly lower ATP consumption). This is achieved by a marked increase of $[Ca^{2+}]_c$-dependent fluxes of the cytosol, including exocytotic insulin secretion (J_{Exo}, A34). As already mentioned, J_{Exo} is now additionally activated by [DAG] to obtain a more pronounced acceleration of this reaction. Such acceleration, however, concomitantly produces a markedly increased ATP consumption, which, at a limited ATP production, might be fulfilled only, when ATP consumption of another ATP utilizing, parallel reaction would be decelerated. The basic idea is that in a network of parallel ATP-coupled fluxes the power output of a given prominent flux can be further increased at a given limited ATP production by depriving ATP power from another less prominent flux of the network, whose power output becomes appropriately reduced at the same time. Such a hierarchy of ATP consuming processes under conditions of ATP deprivation was suggested by Atkinson [28] and experimentally confirmed by Buttgereit and Brand [29].

A $[Ca^{2+}]_c$-independent flux like ATP-dependent protein biosynthesis (J_{Pbs}, A35) appears well suited for such a purpose.

Table 1
$[ATP]_c$ consumption of parallel, $[ATP]_c$-dependent fluxes of the cytosol at steady state and during activation

	$[ATP]_c$ consumption, %								
	[Glu], mM	J_{NaK}	J_{Pbs}	J_{PMCA}	J_{SR2}	J_{Exo}	J_{GK}	J_{SR3}	$5\times J_{IN}$
Fast	4.0	30.87	43.55	19.86	2.74	2.98	3.68	0	0.004
(K_{ATP})	10.0	25.09	26.58	21.05	8.22	18.85	3.73	0	0.23
Slow	4.0	30.78	41.94	19.78	3.61	2.86	3.67	1.03	0.002
(ER)	10.0	27.04	21.30	22.90	9.84	17.99	3.65	0.84	0.10

	J_P, μM/ms	
Fast (K_{ATP})	4.0	0.708
	10.0	1.044
	J_P, μM/ms	
Slow (ER)	4.0	0.709
	10.0	1.005

Abbreviations: NaK = Na-K pump; Pbs = protein biosynthesis; PMCA = Ca^{2+} pump of the cell membrane; SR2 = SERCA2 pump: SR3 = uncoupled SERCA3 pump; Exo = exocytotic insulin release; GK = glucokinase; In = inositol.

3.7. $[Ca^{2+}]_{lu}$ and the IP_3 cycle

It could be convincingly demonstrated that SERCA pumps are involved with β-cell activation [6,7,10]. At a reduced Ca^{2+} filling state of the ER a depolarising I_{CRAN} (A38d) is generated [8,9], which may help to depolarise $\Delta_c\phi$ during a certain period at the beginning of the activation process. Mears et al. [9] could demonstrate that a decreasing filling state of the ER, which was produced by incubations of different durations at low [Glu], was associated with an increasing duration of continuous spiking of $\Delta_c\phi$. The physical link between $[Ca^{2+}]_{lu}$ of the ER and I_{CRAN} (A38a–d) of the cell membrane has not been identified until now, however.

Supposing that the IP_3 cycle would be operative in β-cells, this could provide several potential candidates for flux activation and inhibition, respectively. Supposing further that IP_3 generation from PIP_2 is initiated in β-cells by depolarisation of $\Delta_c\phi$, then IP_3 would be released into the cytosol at the beginning of glucose activation. At the same time DAG is formed in the cell membrane, where it may activate the exocytotic process (J_{Exo}, A34). IP_3 activates on the one hand Ca^{2+} efflux from ER through Ca^{2+} release channels (J_{Rel}, A31), on the other hand, it activates the dephosphorylation of IP_3 to IP_2 and P_i. IP_2 in turn activates further dephosphorylation to In and two P_is (A25–27). Finally, PIP_2 is regained from In and DAG [18] at the expense of five ATPs (J_{IN}, A28).

To construct a link between $[Ca^{2+}]_{lu}$ and IP_3 metabolites in the cytosol, it is suggested that an increased $[Ca^{2+}]_{lu}$ activates dephosphorylation. In the present simulations IP_2 formation

from IP_3 dephosphorylation is selected as an intermediate of the IP_3 cycle (Figs. 2A and 5A), which on the one hand activates J_{CRAN} (A38d) at the cell membrane, and on the other hand inhibits J_{Pbs} (A35) in the cytosol. The mechanism of induction of phosphorylation might be similar to receptor linked activation via G protein cycling. Luminal Ca^{2+} represents the ligand, and a phosphatase at the outer surface of the ER membrane stands for the effector. Soluble phosphatases of the cytosol may then dephosphorylate IP_2 and IP [30].

3.8. The triphasic behaviour of $[Ca^{2+}]_c$

β-cell activation by 10 mM [Glu] induces an increase of the rate of glucose oxidation followed by a change of ATP and ADP species. OP of K_{ATP} channels decreases, $\Delta_c\phi$ depolarises and initiates finally an influx of Ca^{2+} through Ca_V channels [17,31]. These first reactions principally remain unchanged also in the present simulations, but the whole system becomes more complex by the inclusion of ER reactions and the IP_3 cycle. As will be shown these additional reactions are necessary to reproduce experimental observations, especially those of Beauvois et al., Gilon et al., and Arredouani et al. [14,32–34].

In short, this group could demonstrate that SERCA reactions are involved with cytosolic $[Ca^{2+}]_c$ oscillations, and that β-cells possessing, in addition to SERCA2, also SERCA3 Ca^{2+}-ATPase are able to produce compound bursting and mixed $[Ca^{2+}]_c$ oscillations (see below).

To clearly distinguish between the more simple oscillations, in which K_{ATP} channels are functionally involved, and those, which depend on ER reactions, the former oscillations are termed here fast (K_{ATP}) oscillations, and the latter slow (ER) oscillations. Fast (K_{ATP}) oscillations correspond to "simple" and slow (ER) to "slow" oscillations of the Henquin group.

As already mentioned, the first decrease of $[Ca^{2+}]_c$ during glucose activation (phase 0) depends on the action of SERCA pumps. At sub-threshold [Glu]s this decrease of $[Ca^{2+}]_c$ is not observed. In the present simulations phase 0 is brought about by an activation of J_{SR2} (A29) by the glycolytic intermediate, fructose-1,6-biphosphate ([FBP]), which becomes sufficiently elevated at 10 mM [Glu] [10]. The reduction of $[Ca^{2+}]_c$ is produced mainly by J_{PMCA} and J_{SR2} (A33, 29), and is counteracted by an increasingly developing I_{Cav} (B15) (Fig. 1C, D). This activation at a high [Glu] allows Ca^{2+} cycling over the ER membrane to be rather low under resting conditions (4 mM [Glu]), so that ATP wasting by such a futile cycle is low.

When $[Ca^{2+}]_c$ increases above steady state levels (0.17 μM $[Ca^{2+}]_c$) phase 1 begins, $\Delta_c\phi$ shows continuous spiking, and $[Ca^{2+}]_c$ remains elevated until spiking disappears. The increased $[Ca^{2+}]_c$ originates mainly from $[Ca^{2+}]_e$, which entered the cytosol via Ca_V channels as described [cf. 17]. An essential property of J_{SR2} of present simulations is that it is inhibited at a certain elevated $[Ca^{2+}]_{lu}$, so that because of Ca^{2+} inward pumping (J_{SR2}, A29) and release (J_{Rel}, A31), $[Ca^{2+}]_{lu}$ can reach a steady state at a moderately increased $[Ca^{2+}]_{lu}$ and a relative low rate of Ca^{2+} cycling. At a given J_{SR2} the steady state concentration is determined by the conductance G_{Rel}^{max} of J_{Rel}. At $G_{Rel}^{max} = 100$ pS, $[Ca^{2+}]_{lu}$ amounts to 42.5 μM at 4 mM [Glu]. At 10 mM [Glu], $[Ca^{2+}]_{lu}$ oscillates after about 8 min with relative small amplitudes around a value of 275 μM (Fig. 1F).

In addition to the ER reactions IP_3 formation is triggered by a depolarised $\Delta_c\phi$ [6], whereby the IP_3 reaction sequence is initiated. DAG is increased and PIP_2 is lowered. IP_3 activates slightly J_{Rel} (A31), whereby Ca^{2+} accumulation into the ER becomes decelerated. When $[Ca^{2+}]_{lu}$ has exceeded a certain value (about 140 mM), dephosphorylation of IP_3, IP_2, and IP becomes increasingly activated, so that peaks of IP_3 and IP_2 are produced. As mentioned above, the rise of IP_2 has in the present simulations a dual function. On the one hand it activates I_{CRAN} (A38d) to depolarise $\Delta_c\phi$, on the other hand it inhibits J_{Pbs} (A35) to spare ATP. For, a sufficiently increased ATP supply is indispensable for the generation of a prolonged phase of continuous spiking (phase 1) without breaks of repolarisation. I_{CRAN} alone is not sufficient to produce phase 1. It helps to decrease the time needed for $[Ca^{2+}]_{lu}$ accumulation. In addition, J_{CRAN} is involved in slow (ER) oscillations induced by the IP_3 cycle (see below).

Many authors in the field propagate the idea that phase 1 behaviour is induced by I_{CRAN} alone. Magnus and Keizer [35] showed with their model that continuous spiking at the beginning of glucose activation can be initiated by a [Glu]-dependent activation of ATP hydrolysis. A prolonged spiking of $\Delta_c\phi$ could be obtained by delaying the ATP splitting rate. This may be interpreted as an energetic intervention (as in the present simulation), which in addition to electrical stimuli is needed to prolong continuous spiking during phase 1.

In the present model the length of phase 1 depends on the Ca^{2+} filling state of the ER, because it would take a longer time to accumulate Ca^{2+} from a low $[Ca^{2+}]_{lu}$ to a value of about 140 μM, at which dephosphorylation is initiated, than from a high $[Ca^{2+}]_{lu}$.

When $[IP_2]_c$ is sufficiently lowered again, fast (K_{ATP}) oscillations appear, and phase 2 begins. These phase 2 oscillations are very similar (Fig. 1A,B,G,H) to those described recently [17]. As an essential characteristic of this type of oscillation, also fast (K_{ATP}) oscillations do not require activation of phosphofructo kinase (PFK, B1) by $[ADP]_c$. When this activation is omitted, oscillations disappear only in the first part of GLY (J_{GK}, B1, and J_{Al}, B2). Oscillations of all other variables remain preserved. Interestingly, the second part of GLY (J_{Ga}, B4) shows oscillations of decreased amplitudes also under these conditions. When $[Ca^{2+}]_m$ is frozen to 0.23 μM, all oscillations disappear, including those of glycolytic intermediates [cf. 17]. A similar result can be obtained by increasing $1+\kappa_{Cam}$ from 200 to 1000.

3.9. Uncoupling of SERCA3 and the generation of slow (ER) oscillations

Slow oscillations of $[Ca^{2+}]_{lu}$ can be produced by increasing G_{Rel}^{max} (A31) appreciably (not shown). Fridlyand et al. [36] showed with their model that slow oscillations could be produced by an increase of Ca^{2+} efflux from the ER. This was achieved through opening of IP_3-activated Ca^{2+} channels of the ER by an increased $[IP_3]$. To relate an increased Ca^{2+} release to a certain isoform of SERCA pump, which occurs in β-cells, an additional flux through these special pumps is

introduced. It must be uncoupled, however, to produce a Ca^{2+} efflux through the pumps into the cytosol. SERCA3 seems to be a potential candidate for such a purpose, for its K_M of about 2.0 μM [33,37] would suggest that this isoform is less essentially involved with Ca^{2+} pumping into the ER compared with SERCA2b, which is known to have a much lower K_M for $[Ca^{2+}]_c$.

Derivation of the uncoupled SERCA3 flux equation:

In non-equilibrium thermodynamics coupled reactions are described by the following equations:

$$J_1 = L_{11} \cdot X_1 + L_{12} \cdot X_2, \quad \text{and} \quad J_2 = L_{12} \cdot X_1 + L_{22} \cdot X_2 \tag{1a, 1b}$$

[38–40]. J_1 and J_2 are defined as the output and input fluxes, respectively, and X_1 and X_2 are the output and input conjugated thermodynamic forces. L_{11} and L_{22} are the straight coefficients, and L_{12} represents the coupling coefficient. The degree of such a direct coupling (in contrast to indirect uncoupling through a parallel membrane leak) is defined as $q = L_{12}/\sqrt{L_{11} \cdot L_{22}}$, the phenomenological stoichiometry as $Z = \sqrt{L_{11}/L_{22}}$.

According to Weiss [41], this concept may be described by an electrical network analogue having two batteries with opposite voltages U_1 and U_2 (U_1 negative), one coupling conductance G_3, and two leak conductances G_1 and G_2. The output current I_1 and the input current I_2 are given by $I_1 = G_3((\lambda_1+1)U_1+U_2)$, and $I_2 = G_3(U_1+(\lambda_1+1)\ U_2)$, ($\lambda_1 = G_1/G_3$ and $\lambda_2 = G_2/G_3$). By comparison with Eqs. (1a) and (1b), it turns out that $q = 1/\sqrt{(\lambda_1+1)\cdot(\lambda_2+1)}$, and $Z = \sqrt{(\lambda_1+1)/(\lambda_2+1)}$.

Uncoupling Ca^{2+} transport (output flux) of the SERCA3 Ca^{2+} pump reaction from ATP splitting in analogy to the equation for I_1 yields

$$J_{SR3} = \alpha_c \times G_{SR3} \times \left((\lambda_{SR3ca} + 1) \times \frac{RT}{F} \ln\left(\frac{[Ca^{2+}]_c^2}{[Ca^{2+}]_r^2} \frac{[H^+]_r^4}{[H^+]_c^4} + \tilde{A}_{ATPc} \right) \right) \tag{2}$$

($\tilde{A}_{ATPc}$ denotes $-\Delta_r G'(ATP_c)$ in mV, A5, 11).

It seems noteworthy to mention that the above flux equation was derived assuming that 2.0 Ca^{2+} and 2.0 H^+ ions are transported per split ATP molecule under coupled conditions, and that two protons leave the ER lumen at the same time separately and at the same velocity through proton channels of the ER membrane. Under such conditions both reactions can be understood as proceeding in series with their own individual conductances and driving forces. They are contracted to one single reaction with conductance G_{SR3} and driving force A_{SR3} (Eq. (2)). ER membrane potentials of the contracted driving force cancel and four protons instead of two are released per cycle. J_{PMCA} (A33) at the cell membrane was treated in an analogous manner. As a result, these contracted reactions are not electrogenic.

Uncoupling of J_{SR3} causes an additional release of Ca^{2+} from the ER via SERCA3 pumps. The effect of such an uncoupling at $\lambda_{R3ca} = 5$ is shown in Fig. 5E. Obviously, fast (K_{ATP}) oscillations are replaced by much slower oscillations (Figs. 4 and 5), which differ from the latter in several aspects. Most noticeable, under these conditions slow (frequency $\nu = 0.177$ 1/min) oscillations of $[Ca^{2+}]_{lu}$ having high amplitudes are produced (Fig. 4F). $[ADP]_c$ (and G_{Katp}, A40) oscillations are now in phase with bursts of $\Delta_c\phi$ and $[Ca^{2+}]_c$ oscillations (Fig. 4G). These slow (ER) oscillations are initiated in the same way as the triphasic $[Ca^{2+}]_c$ oscillations described above: after an increase of [Glu] above 7.0 mM, $[ADP]_c$ becomes reduced, $\Delta_c\phi$ depolarises, and $[Ca^{2+}]_c$ increases. However, instead of passing from phase 1 into fast (K_{ATP}) oscillations, a long lasting silent phase begins. This phase is not related to an increase of $[ADP]_c$, but is brought about by pronounced oscillations of $[Ca^{2+}]_{lu}$ and all constituents of the IP_3 cycle, especially of $[IP_2]$, because dephosphorylation of IP_2 (and IP) is kinetically coupled to $[Ca^{2+}]_{lu}$ (Fig. 5A). On the other hand, $[IP_2]$ activates I_{CRAN} (A38d) and depolarises $\Delta_c\phi$, so that bursts and elevations of $[Ca^{2+}]_c$ are practically in phase (Fig. 4G). Peaks of $[ADP]_c$ are also in phase with these slow (ER) oscillations, but cannot induce repolarisation, because they obviously take place at a too low level ($[ADP]_c^{tam} = 174$ μM). The lowered $[ADP]_c$ production is caused by the additional Ca^{2+} leakage through SERCA3, which initiates $[Ca^{2+}]_{lu}$ oscillations. Thereby $[IP_2]$ is forced to oscillate at a more elevated level than without $[Ca^{2+}]_{lu}$ oscillations (for comparison see Figs. 5A and 2A), so that J_{Pbs} (A35) inhibition is more pronounced and, as a result, total $[ATP]_c$ consumption (J_P, A36) finally becomes reduced.

That $[ADP]_c$ and hence K_{ATP} channels are not involved with slow (ER) oscillations except during initiation, can be taken from the fact that $[Ca^{2+}]_m$ activation of mitochondrial metabolism (J_{PDH}, A23, J_{CAC}, A24) is not an indispensable requirement for slow (ER) oscillations. Under conditions of Figs. 4 and 5, inhibition of Ca^{2+} cycling over the inner membrane freezes matrix $[Ca^{2+}]_m$ to 0.23 μM, but does not impair oscillations (not shown). Moreover, also an increase of $1+\kappa_{Cam}$ from 200 to 5000 does practically not change oscillatory behaviour. Obviously, under conditions of slow (ER) oscillations amplitudes, especially of $[Ca^{2+}]_c$ oscillations are not considerably altered [cf. 42]. Only J_{HCE} (B12) is slightly delayed (out of phase) compared to J_{CU} (B11), so that amplitudes of pH_m oscillations become reduced.

In contrast to fast (K_{ATP}) oscillations, slow (ER) oscillations require PFK activation by $[ADP]_c$. Without PFK activation the system is transferred into a state of continuous spiking (not shown).

3.10. Compound bursting and mixed $[Ca^{2+}]_c$ oscillations

In a recent experimental study, Beauvois et al. [14] could demonstrate that mixed $[Ca^{2+}]_c$ oscillations in mouse β-cells result from so-called compound bursting of $\Delta_c\phi$. Compound bursting is characterised by oscillations of $\Delta_c\phi$ occurring in several bursts of variable length, so-called bouts, which are separated by prolonged silent intervals. These authors showed further that compound bursting and mixed oscillations of $[Ca^{2+}]_c$ could be initiated only with β-cells, which possessed SERCA3 Ca^{2+} pumps. Ablation of SERCA3 was not compensated for by other SERCA isoforms, including the main isoform of β-cells SERCA2b [33].

These types of oscillations are fairly well reproduced by a simulation, which includes also uncoupling of SERCA3 like

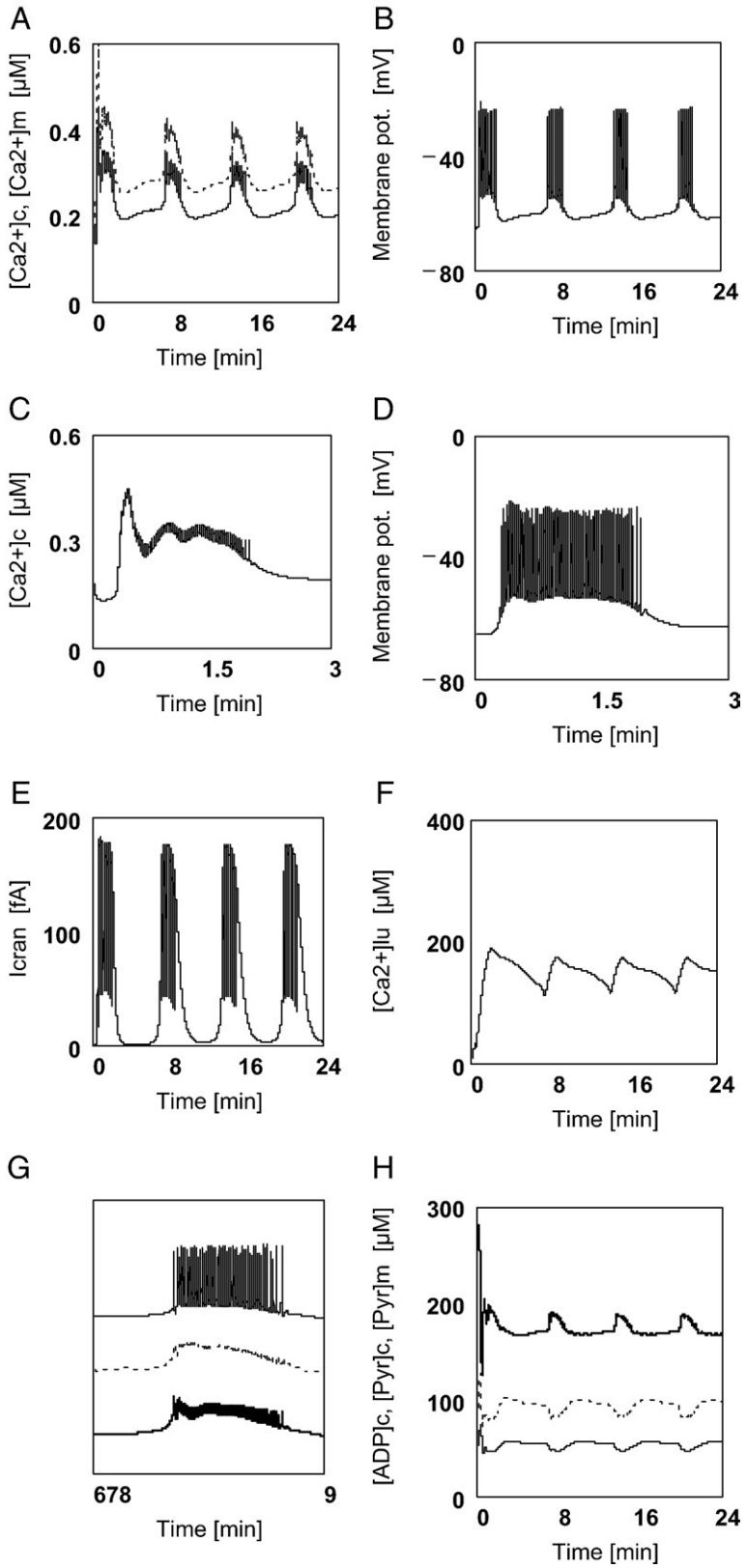

Fig. 4. Slow (ER) oscillations at 10 mM [Glu]. (A) (line) $[Ca^{2+}]_c$; (dot) $[Ca^{2+}]_m$. (B) (line) $\Delta_c\phi$. (C) (line) $[Ca^{2+}]_c$ phases during first 3 min. (D) (line) $\Delta_c\phi$ during first 3 min. (E) (line) I_{CRAN}. (F) (line) $[Ca^{2+}]_{lu}$. (G) (line) $\Delta_c\phi$; (dot) G_{Katp}; (bold line) $[Ca^{2+}]_c$, ordinates of $\Delta_c\phi$ and $[Ca^{2+}]_c$ are transformed to be comparable with G_{Katp}. (H) (bold line) $[ADP]_c$; (dot) $[Pyr]_m$; (line) $[Pyr]_c$.

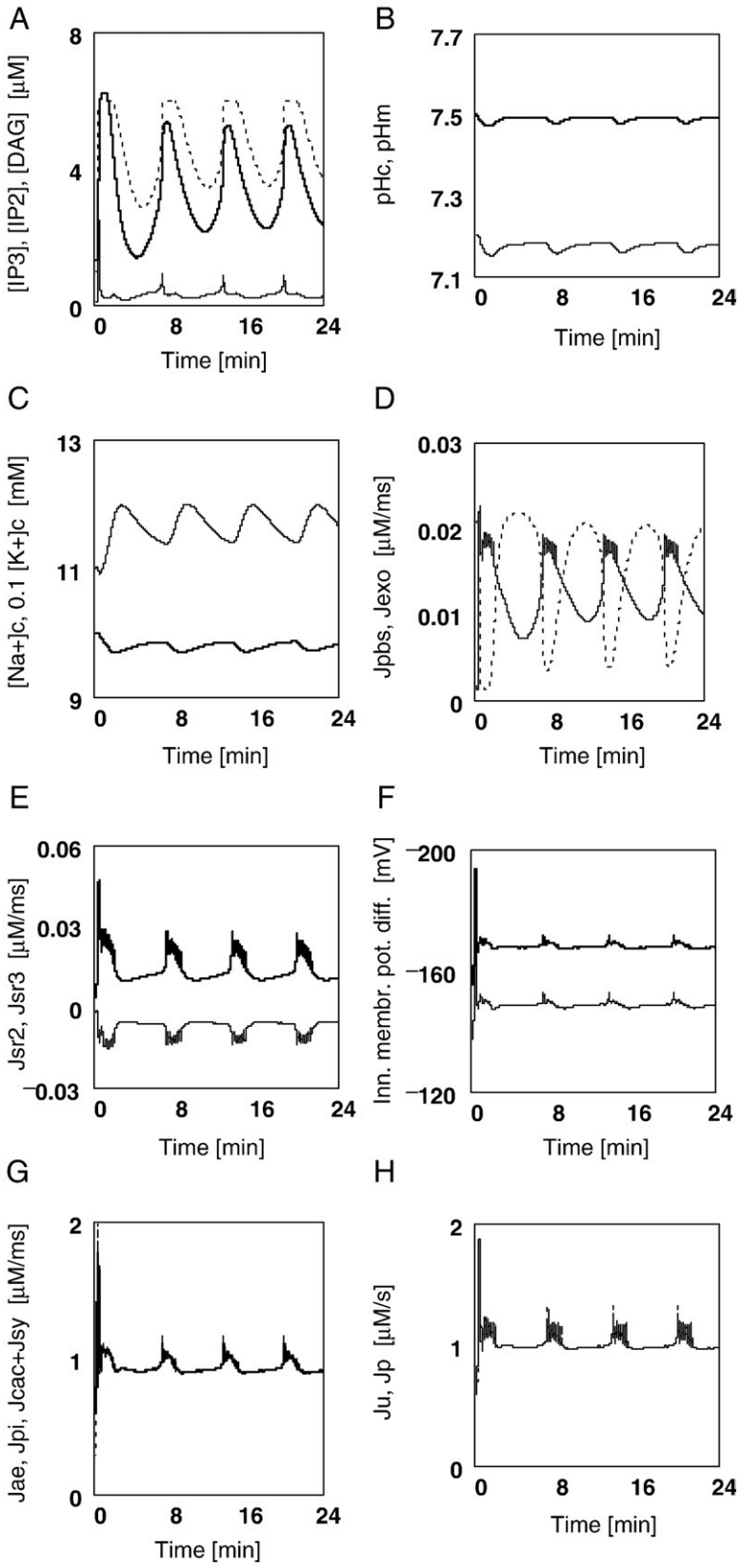

Fig. 5. Slow (ER) oscillations at 10 mM [Glu]. (A) (dot) DAG; (bold line) IP_2; (line) IP_3. (B) (bold line) pH_m; (line) pH_c. (C) (line) $[Na^+]_c$; (bold line) $[K^+]_c$. (D) (dot) J_{Pbs}; (line) J_{Exo}. (E) (bold line) J_{SR2}; (line) J_{SR3}. (F) (bold line) $\Delta\,\tilde{\mu}_H$; (line) $\Delta_m\phi$. (G) (bold line) J_{AE}; (line) J_{Pi}; (dot) J_{CAC} plus J_{SY}. (H) (line) J_U; (dot) J_P.

that for slow (ER) oscillations, in which, however, IP_2-dependent deactivation of protein biosynthesis is omitted (deactivation factor = 1.0, A35), PDH conductance is reduced (A23), or by reducing redox shuttles. Fig. 6 shows compound bursting and mixed $[Ca^{2+}]_c$ oscillations brought about by omitting J_{MS} (B7a) and by reducing the maximal conductance

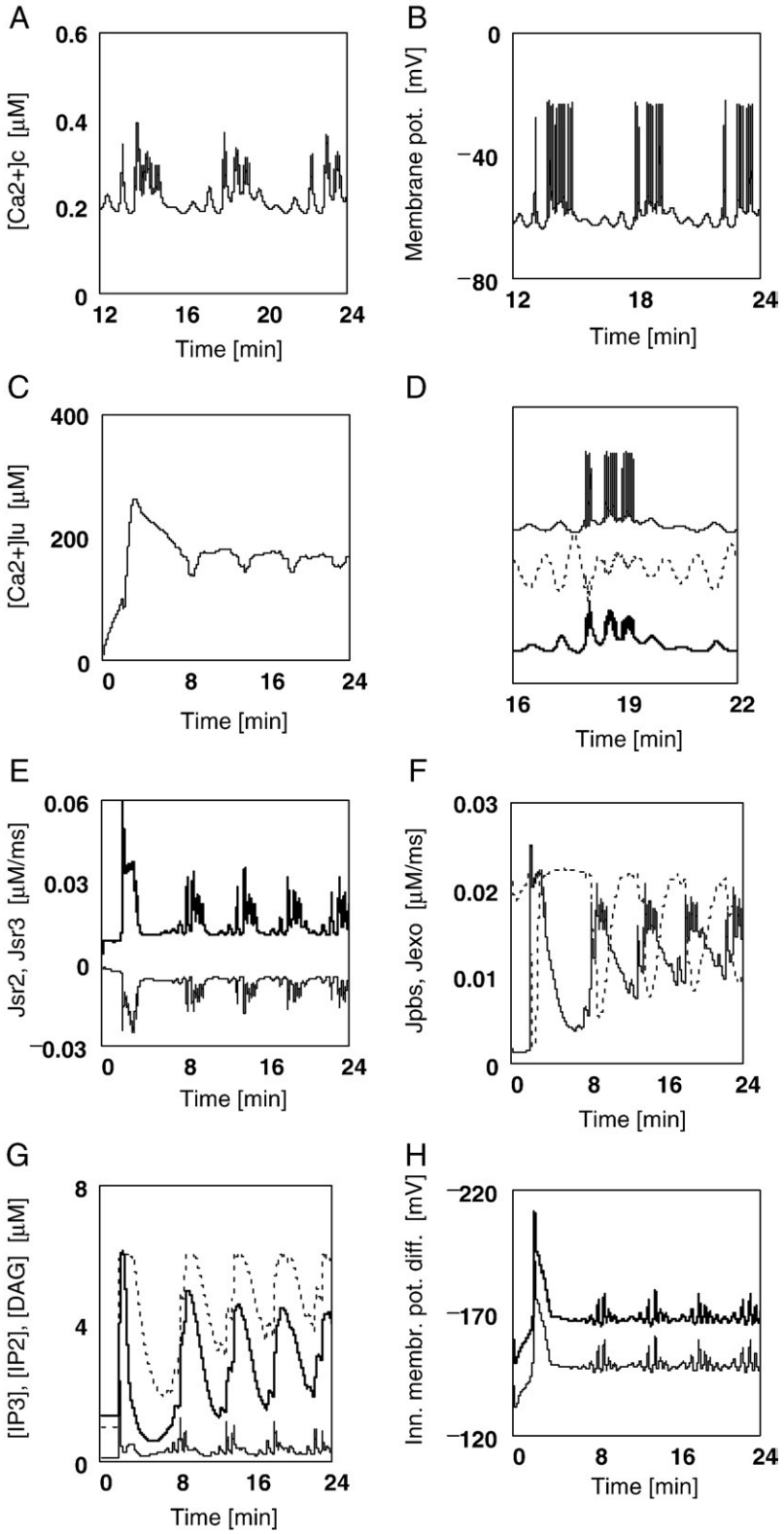

Fig. 6. Compound bursting and mixed oscillations at 10 mM [Glu]. (A) (line) $[Ca^{2+}]_c$. (B) (line) $\Delta_c\phi$. (C) (line) $[Ca^{2+}]_{lu}$. (D) (line) $\Delta_c\phi$; (dot) G_{Katp}; (bold line) $[Ca^{2+}]_c$, ordinates of $\Delta_c\phi$ and $[Ca^{2+}]_c$ are transformed to be comparable with G_{Katp}. (E) (bold line) J_{SR2}; (line) J_{SR3}. (F) (dot) J_{Pbs}; (line) J_{Exo}. (G) (dot) DAG; (bold line) IP_2; (line) IP_3. (H) (bold line) $\Delta\tilde{\mu}_H$; (line) $\Delta_m\phi$.

of J_{GS} to $0.85 \times G_{GS}^{max}$ (B6). This indicates that a reduced availability of $[ATP]_c$ may be functionally involved, confirming results of Beauvois et al. [14], who found that compound bursting and mixed $[Ca^{2+}]_c$ oscillations could be best initiated at a slightly reduced but still activating [Glu] of 8.0 mM. In simulations, however, a reduction of [Glu] alone was ineffective to yield these effects, perhaps because [Glu] in present oscillations is a fixed parameter, whereas it can oscillate under experimental conditions [43].

During silent phases low amplitude oscillations come into view, which behave similar to fast (K_{ATP}) oscillations. From Fig. 6D it can be taken that oscillations of $[ADP]_c$ and $\Delta_c\phi$ indeed show the phase behaviour of fast (K_{ATP}) oscillations, that is, peaks of $[ADP]_c$ are in phase with silent phases of $\Delta_c\phi$ and $[Ca^{2+}]_c$. The bouts of $\Delta_c\phi$ go along with elevations of $[ADP]_c$ and $[Ca^{2+}]_c$, but are less pronounced when compared to the results of Beauvois et al. [14]. When $[Ca^{2+}]_m$ is frozen at a value of 0.23 μM, slow oscillations appear, which are similar to slow (ER) oscillations, but are less pronounced, and bursting of $\Delta_c\phi$ has vanished. Obviously, compound bursting and mixed $[Ca^{2+}]_c$ oscillations at a decreased $[ATP]_c$ availability are possible only, when mitochondria can be activated by $[Ca^{2+}]_m$ (J_{PDH}, A23, and J_{CAC}, A24). Slow (ER) oscillations, on the other hand, are entirely independent of such an activation. It may be concluded, therefore that compound bursting and mixed $[Ca^{2+}]_c$ oscillations are brought about by a superposition of slow (ER) and fast (K_{ATP}) oscillations.

Slow (ER) oscillations are fundamentally different from those slow oscillations presented recently [cf. 17]. Such oscillations could be produced by appreciably reducing the flux through PDH plus CAC. A very similar behaviour can be obtained here with fast (K_{ATP}) oscillations by reducing PDH conductance to $0.15 \times L_{PDH}^{max}$ (A23, not shown). Slow (ER) oscillations, however, pass over at this conductance into fast (K_{ATP}) oscillations, because under these conditions $[ADP]_c$ becomes much more elevated, so that now K_{ATP} channels (A40) are involved again with the generation of oscillations. Large $[Ca^{2+}]_{lu}$ oscillation disappears under these conditions. At a more moderate reduction of PDH conductance to $0.53 \times L_{PDH}^{max}$, as mentioned already, mixed $[Ca^{2+}]_c$ oscillations appear. $[ADP]_c^{tam}$ is slightly increased from 174 to 176 μM, $[Ca^{2+}]_{lu}$ shows large amplitude oscillations, but compound bursting of $\Delta_c\phi$ can be recognised only at the base.

Bertram et al. [12] demonstrated with their model that slow oscillations are due to glycolytic oscillations, whereas fast oscillations are related to their electrical Ca^{2+} model of oscillations. Compound bursting can be produced by superimposing fast on slow glycolytic oscillations. A serious drawback, however, of their model is given by the fact that the flux equations violate the stoichiometry of oxidative glucose metabolism: the quotient of O_2 consumption and glucose utilisation (J_O/J_{GK}, [12]) amounts only to 0.75 to 1.2 instead of 6.0. ATP output and associated $[ADP]_c$ production therefore must be rather weak, so that glycolytic oscillations brought about by an autocatalytic PFK reaction may be facilitated. Moreover, coupled ATP and NAD_{red} production by GLY were not considered, which seriously truncates glucose metabolism.

If, however, $[ATP]_c$ production were much more pronounced, and moreover, all cytosolic $[ATP]_c$ consuming reactions would be responsible for $[ADP]_c$ formation, as it is known for intact cells, then the flux through PFK would be merely 3.7% of total $[ADP]_c$ production (J_{GK}/J_P, see Table 1, B1, A36). In other words, PFK-induced oscillations can be expected only, if the predominant part of $[ATP]_c$ production would be accomplished solely by GLY. Therefore, autocatalysis and generation of oscillations by this single reaction step alone seems to be rather improbable. Thus, oscillations of glycolytic intermediates under physiological conditions can be mediated and possibly reinforced, but probably are not generated by the PFK reaction. This applies for both fast (K_{ATP}) and for slow (ER) oscillations of the present simulations.

4. Summary and conclusions

For the treatment of cation homeostasis, it is imperative to include J_{NaK} into simulations. At a given steady state loss of $[K^+]_c$ through K_{ATP} channels, J_{NaK} has to be of sufficient magnitude in order to avoid a serious reduction of $[K^+]_c$. The associated outward current has to be balanced by an adequate Na^+ inward current. Under such conditions J_{NaK} does not disturb electrical and energetic processes associated with conditions of β-cell rest and activity, so that J_{NaK} is not directly involved with production of oscillations.

It has been shown by introducing binding polynomials that the decrease of pH during β-cell activation is only small, and, moreover does not affect cellular energetics or opening behaviour of the K_{ATP} channel. However, pH-dependent changes of $[Mg^{2+}]_c$ might be sufficient to produce an appreciable alteration of $[ADP]_c$ and $[ATP]_c$ species, which in turn might interfere with the channel's OP. It seems plausible therefore to suggest that this channel is additionally controlled by pH_c to counteract such unwanted $[Mg^{2+}]_c$-evoked effects.

For the triphasic patterns of fast (K_{ATP}) oscillations, additional ER reactions are necessary. The Ca^{2+} filling state of the ER is signalled to the cell membrane by IP_2, an intermediate of the IP_3 cycle, which triggers depolarisation of $\Delta_c\phi$, which in turn can prolong the first bursting phase of $\Delta_c\phi$. This is supported by an additional transient inhibition of J_{Pbs} through IP_2, to increase $[ATP]_c$ availability. The first decrease of $[Ca^{2+}]_c$ at the beginning of glucose activation is achieved by activation of J_{SR2} by FBP.

For the induction of slow (ER) oscillations, β-cells must additionally possess the isoform SERCA3, which, when sufficiently uncoupled, allows Ca^{2+} leakage from the ER into the cytosol. This additional leak flux initiates oscillations of $[Ca^{2+}]_{lu}$, and, thereby, oscillations of $[Ca^{2+}]_c$ through the mediation of the IP_3 cycle. $[ADP]_c$ and K_{ATP} do not participate with the generation of slow (ER) oscillations.

All oscillations presented here are generated by interacting metabolite and/or Ca^{2+} cycles. It is concluded that PFK, as a putative glycolytic oscillator, is not causally involved with the generation of oscillations, because $[ATP]_c$ consumption by the PFK reaction alone is too low compared to parallel $[ATP]_c$ utilisation, to generate oscillations of glycolytic intermediates by autocatalysis.

Appendix A

The new mathematical simulations presented here are founded on those given in my recent article [cf. 17]. In section "A" all new equations are listed, whereas section "B" contains taken over equations. Explanations about these latter equations are to be found in that article.

One additional variable of glucose metabolism, acetyl coenzyme A, is included to allow input of fatty acid metabolites from β oxidation (not treated here). As a further modification, pH_m is lowered from 7.7 to 7.5.

A. New equations

pH and pMg dependent ATP hydrolysis

In biochemistry Gibbs free energy of ATP hydrolysis usually is expressed as

$$\Delta_r G' = -RT\ln K' + RT\ln\Gamma', \text{ and } K' = \frac{[\mathrm{ADP}]_{eq}[P_i]_{eq}}{[\mathrm{ATP}]_{eq}[c^0]}. \tag{A1}$$

$[c^0]$=unit concentration to make a logarithmic argument dimensionless, Γ' denotes the corresponding mass action quotient of non-equilibrium concentrations. K' depends on $[H^+]$ and $[Mg^{2+}]$. To obtain an expression for $\Delta_r G'$, which contains already these dependencies, K' has to be related to a reference constant K^{ref} in chemical notation:

$$K^{ref} = \frac{\left[\mathrm{ADP}^{3-}\right]_{eq}\left[\mathrm{HPO}_4^{2-}\right]_{eq}[\mathrm{H}^+]_{eq}}{\left[\mathrm{ATP}^{4-}\right]_{eq}[c^0]^2} \quad \text{(Alberty, [1]).} \tag{A2}$$

From this K^{ref} another reference constant can be derived by replacing $[HPO_4^{2-}]_{eq}[H+]_{eq}$ by $[H_2PO_4^-]_{eq}$ yielding

$$K^{ref1} = \frac{\left[\mathrm{ADP}^{3-}\right]_{eq}\left[\mathrm{H_2PO_4^-}\right]_{eq}}{\left[\mathrm{ATP}^{4-}\right]_{eq}[c^0]}, \tag{A3}$$

$K^{ref1} = K^{ref}/K1pi = 2.2666\times10^5$ ($K1pi$=first dissociation constant of $H_2PO_4^-$).

Introducing this latter constant yields

$$\Delta_r G' = -RT\ln\left(K^{ref1}\times\frac{P_{ADP3-}P_{H2PO4-}}{P_{ATP4-}}\right) + RT\ln(\Gamma'), \text{ or} \tag{A4}$$

$$A_{ATP} = RT\ln\left(K^{ref1}\times\frac{P_{ADP3-}P_{H2PO4-}}{P_{ATP4-}}\times\frac{1}{\Gamma'}\right). \tag{A5}$$

This equation considers influences of $[H^+]$ and $[Mg^{2+}]$ on $\Delta_r G'$ through introduction of $[H^+]$- and $[Mg^{2+}]$-dependent polynomials and K^{ref1} for K'. The Ps denote so-called binding polynomials (see Alberty, [1]). The indices of binding polynomials indicate the species towards which polynomials are evolved.

The following binding polynomials were used in equations of ATP hydrolysis, the ATP cycle, and conductance of K_{ATP} channel:

$$P_{ATP4-} = 1 + \frac{[\mathrm{H}^+]}{K1at} + \frac{[\mathrm{H}^+]^2}{K1at\,K2at} + \frac{[\mathrm{Mg}^{2+}]}{K3at} + \frac{[\mathrm{Mg}^{2+}][\mathrm{H}^+]}{K1at\,K4at} + \frac{[\mathrm{Mg}^{2+}]^2}{K3at\,K5at}. \tag{A6}$$

$$P_{ADP3-} = 1 + \frac{[\mathrm{H}^+]}{K1ad} + \frac{[\mathrm{H}^+]^2}{K1ad\,K2ad} + \frac{[\mathrm{Mg}^{2+}]}{K3ad} + \frac{[\mathrm{Mg}^{2+}][\mathrm{H}^+]}{K1ad\,K4ad}. \tag{A7}$$

$$P_{MgADP-} = P_{ADP3-}\times\frac{K3ad}{[\mathrm{Mg}^{2+}]}. \tag{A8}$$

$$P_{HPO4--} = 1 + \frac{[\mathrm{H}^+]}{K1pi} + \frac{[\mathrm{Mg}^{2+}]}{K2pi}. \tag{A9}$$

$$P_{H2PO4-} = P_{H2PO4--}\times\frac{K1pi}{[\mathrm{H}^+]}. \tag{A10}$$

Constants were taken from Alberty [1]. They are here related to proton activity (10^{-pH}) at 0.25 M ionic strength.

Fluxes of the mitochondrial ATP cycle

All fluxes of the ATP cycle contain now pH and pMg dependent binding polynomials.

The flux through F_1F_0-ATPase is given by

$$J_{SY} = \alpha_m \cdot v_s \cdot \frac{[ADP]_m^2}{(K_M^{SY})^2 + [ADP]_m^2} \cdot G_{SY}^{max} \times \left(-\tilde{A}_{ATPm} + \frac{1}{v_s}\left(\frac{RT}{F} \ln\left(\frac{[H^+]_c}{[H^+]_m} \right) - \Delta_m\phi \right) \right), \tag{A11}$$

$\tilde{A}_{ATPc} = A_{ATPc}/F$, $\tilde{A}_{ATPc}$, and RT/F are given in mV throughout, $K'_{ATPm} =$. $K_M^{SY} = 500$ μM, $G_{SY}^{max} = 760$ pS, $v_s = 1/3$.

The flux through proton/phosphate symport is given by

$$J_{Pi} = \alpha \times G_{Pi}^{max} \times RT \ln\left(\frac{P_{H2PO4-}^m}{P_{H2PO4-}^c} \frac{[Pi]_c}{[Pi]_m} \frac{[H^+]_c}{[H^+]_m} \right), \tag{A12}$$

and through the adenine nucleotide exchange reaction by

$$J_{AE} = \alpha \times \frac{[ADP]_c^2}{(K_M^{AE})^2 + [ADP]_c^2} \times G_{AE}^{max} \times \left(\frac{RT}{F} \ln\left(\frac{P_{ATP4-}^c}{P_{ATP4-}^m} \frac{P_{ADP3-}^m}{P_{ADP3-}^c} \frac{[ATP]_m}{[ATP]_c} \frac{[ADP]_c}{[ADP]_m} \right) - \Delta_m\phi \right), \tag{A13}$$

$G_{Pi}^{max} = 4560$ pS, G_{AE}^{max} is reduced from 1140 to 80 pS to make $\Delta_m\phi$ more negative. $K_M^{AE} = 20$ μM.

Buffering and fluxes of CO_2

To obtain an expression for the time derivative of proton activity, from which $[H^+]$ can be computed, the following relation is used:

$$\frac{d[H^+]_{tot}}{dt} = \frac{d[H^+]}{dt} + \frac{d[H^+]_{bound}}{dt}$$

($[H^+]$="free" proton activity). The left hand term is given by the sum of all proton producing and consuming reactions of a given compartment, $\Sigma v_i J_i$ (v_i=stoichiometric coefficients of produced (+) or consumed (−) protons). One possibility to yield this derivative would be given by including $d[H^+]_{bound}/dt$ into the sum of proton consuming reactions. Another way is given by

$$\frac{d[H^+]_{bound}}{dt} = \kappa^{BU} \times \frac{d[H^+]}{dt}, \text{yielding} \tag{A14}$$

$$\frac{d[H^+]}{dt} = \frac{1}{1 + \kappa^{BU}} \times \sum v_i J_i. \tag{A15}$$

$$\kappa^{BU} = [BU_{tot}] \frac{K_D^{BU}}{(K_D^{BU} + [H^+])^2} \text{is used [44],}$$

K_D^{Bu}=dissociation constant of intrinsic buffer BU. According to [21] two intrinsic buffers were supposed having the following constants: $K_{D1}^{BU} = 10^{-0.03}$ μM, $K_{D2}^{BU} = 10^{-1.57}$ μM, $[BU_{tot}^1] = 84.22 \times 10^3$ μM, $[BU_{tot}^2] = 29.38 \times 10^3$ μM.

From the definition $\beta = -d[H^+]_{tot}/d\text{pH}$, it follows,

$$\beta^{Bu} = \ln(10)\ [H^+]\left(1 + \kappa_H^{Bu}\right). \tag{A16}$$

Because one variable can be spared by the latter formulation, this is used in simulations throughout. This implies, however, that intrinsic buffers react with high velocities, since they are treated in computations as an at once process. Because the flux through carboanhydrase, (J_{CA}), probably proceeds at a much lower velocity, it is included in $\Sigma v_i J_i$ and, therefore, does not appear as an additional κ_H^{CO2} in the denominator of Eq. (A14).

CO_2 permeation of the mitochondrial inner membrane and of the cell membrane are given by

$$J_{CO2m} = \alpha_m \times G_{CO2m}^{max} \times \frac{RT}{F} \ln\left(\frac{[CO_2^{aq}]_m}{[CO_2^{aq}]_c} \right), \quad \text{and} \tag{A17a}$$

$$J_{CO2c} = \alpha_c \times G_{CO2c}^{max} \times \frac{RT}{F} \ln\left(\frac{[CO_2^{aq}]_c}{[CO_2^{aq}]_e} \right), \tag{A17b}$$

$G^{max}_{CO2m}=6.7\times10^5$ pS, $G^{max}_{CO2c}=0.287\times G^{max}_{CO2m}=1.9\times10^5$. The surface of the cell membrane is by a factor of 0.287 smaller than mitochondrial membranes of a cell. The factor can be obtained by building the quotient from capacitances of the cell membrane and mitochondrial membranes 5309 fF / 18,493 = 0.287 fF (fF = femtofarad, see [cf. 17]).

Fluxes of CO_2 and HCO_3 through the CA catalysed reaction is given by

$$J_{CAm}=\frac{\left[HCO_3^-\right]_m^3}{\left(K_M^{CA}\right)^3+\left[HCO_3^-\right]_m^3}\times L^{max}_{CAm}\times RT\ln\left(\frac{\left[CO_2^{aq}\right]_m}{\left[HCO_3^-\right]_m[H^+]_m}\times K_{CO2}\right),\quad\text{and} \tag{A18a}$$

$$J_{CAc}=\frac{\left[HCO_3^-\right]_c^3}{\left(K_M^{CA}\right)^3+\left[HCO_3^-\right]_c^3}\times L^{max}_{CAc}\times RT\ln\left(\frac{\left[CO_2^{aq}\right]_c}{\left[HCO_3^-\right]_c[H^+]_c}\times K_{CO2}\right). \tag{A18b}$$

$$L^{max}_{CO2m}=L^{max}_{CO2c}=10^{-4},\quad K_{CO2}=10^{-6.17}\times10^6\,\mu M=0.676\,\mu M,\quad K_M^{CA}=2.0\times10^3.$$

ATP cycling and proton binding

The line integral (LI) over the closed path of all potential differences of ATP must vanish. $LI=A_{ATPc}-A_{ATPm}-A_{AE}+A_{Pi}-(-\Delta\tilde{\mu}_H)$. One negative $\Delta\tilde{\mu}_H$ has to be subtracted, because it was included in the driving forces of coupled reactions of J_{AE} plus J_{Pi}.

$$A_{AE}+A_{Pi}-(-\Delta\tilde{\mu}_H)=RT\ln\left[\frac{\left[ATP^{4-}\right]_m[c^0]}{\left[ADP^{3-}\right]_m\left[H_2PO_4^-\right]_m}\right]+RT\ln\left[\frac{\left[ADP^{3-}\right]_c\left[H_2PO_4^-\right]_c}{\left[ATP^{4-}\right]_c[c^0]}\right]. \tag{A19}$$

Adding $A_{ATPc}-A_{ATPm}$ (chemical notation) yields

$LI=RT\ln K_c^{refl}-RT\ln K_m^{refl}=0$ (both constants are equal).

The change of H^+ binding must also vanish, because

$$\Delta_r N_H=\left(\frac{\partial\ln K^{refl}}{\partial\ln[H^+]}\right)_{[Mg^{2+}]}=0. \tag{A20}$$

In contrast to K', K^{refl} does not depend on pH [cf. 1], that is, during cycling of ATP protons are whether produced neither consumed by cycling. This applies to the cytosol as well as to the mitochondrial matrix.

pH_c control by cell membrane reactions

The primary mechanism to counteract intracellular acidification is given by the Na^+/H^+ exchange reaction of the cell membrane. The flux through this reaction is given by

$$J_{NHE}=\alpha_c\times\frac{1}{1+\exp\left(\frac{\left[H_h^+\right]_{NHE}-[H^+]_c}{[S_{NHE}]}\right)}\times G^{max}_{NHE}\times\frac{RT}{F}\ln\left(\frac{[Na^+]_e}{[Na^+]_c}\,\frac{[H^+]_c}{[H^+]_e}\right). \tag{A21}$$

$$G^{max}_{NHE}=100\text{ pS},\ \left[H_h^+\right]_{NHE}=0.0727\,\mu M,\quad [S_{NHE}]=0.007\,\mu M.$$

Intracellular alkalinisation is counteracted by the anion exchange reaction of the cell membrane. The flux through this reaction is given by

$$J_{AnE}=\alpha_c\times\frac{1}{1+\exp\left(\frac{[H^+]_c-\left[H_h^+\right]_{AnE}}{[S_{AnE}]}\right)}\frac{\left[HCO_3^-\right]_c^2}{\left(K_M^{AnE}\right)^2+\left[HCO_3^-\right]_c^2}\times G^{max}_{AnE}\times\frac{RT}{F}\ln\left(\frac{[CL^-]_e}{[CL^-]_c}\,\frac{\left[HCO_3^-\right]_c}{\left[HCO_3^-\right]_e}\right), \tag{A22}$$

$$G^{max}_{AnE}=180\text{ pS},\left[H_h^+\right]_{AnE}=0.0159\mu M,\quad [S_{AnE}]=0.008\mu M, K_M^{AnE}=15\times10^3.$$

Additional fluxes of glucose metabolism

Present simulations contain the PDH reaction given by

$$J_{PDH}=\frac{\left(K_I^{PDH}\right)^4}{\left(K_I^{PDH}\right)^4+[NAD_{red}]_m^4}\times\frac{\left[Ca^{2+}\right]_m^2}{\left(K_M^{Cam}\right)^2+\left[Ca^{2+}\right]_m^2}\times\frac{[Pyr]_m^3}{\left(K_M^{Pym}\right)^3+[Pyr]_m^3}\times L^{max}_{PDH}$$
$$\times\ RT\ln\left[\frac{[NAD_{ox}]_m}{[NAD_{red}]_m}\,\frac{[AcCoA_{ox}]_m}{[AcCoA_{red}]_m}\,\frac{[Pyr]_m}{[CO_2^{aq}]_m}\times K'_{PDH}\right], \tag{A23}$$

$L^{max}_{PDH}=8.34\times10^{-5}$(μM/ms)×(mol/J), $K'_{PDH}=2.3602\times10^{6}$, the constant for PDH inhibition by NAD_{red} is set to $K_I=10$ μM. CO_2^{aq} denotes dissolved CO_2 (single species). Total acetyl-coenzyme A concentration of the matrix, $[AcCoA_{tot}]_m$, is set to 130 μM.

All following reactions of the citric acid cycle were contracted to one single step yielding

$$J_{CAC}=\frac{(K_I^{PDH})^4}{(K_I^{PDH})^4+[NAD_{red}]_m^4}\times\frac{[Ca^{2+}]_m^2}{(K_M^{Cam})^2+[Ca^{2+}]_m^2}\times\frac{[AcCoA_{red}]_m^2}{(K_M^{AcC})^2+[AcCoA_{red}]_m^2}\times L^{max}_{CAC}$$
$$\times RT\ln\left[\frac{[NAD_{ox}]_m^3}{[NAD_{red}]_{m3}^3}\frac{[FAD_{ox}]_m}{[FAD_{red}]_m}\frac{[AcCoA_{red}]_m}{[AcCoA_{ox}]_m}\frac{[c^0]^2}{[CO_2^{aq}]_m^2}\frac{[ADP]_m[Pi]_m}{[ATP]_m[c^0]}\times K'_{CAC}\right], \tag{A24}$$

$L^{max}_{CAC}=1.938\times10^{-5}(\mu M/ms)\times(mol/J), K'_{CAC}=1.3536\times10^{11};\quad K_M^{AcC}=60$ μM.

All other fluxes of glucose metabolism, constants and explanations are given in ref. [17].

IP_3 cycle

The IP_3 cycle in the present simulations is activated by depolarisation. This is enabled by the first activation factor. Flux through phospholipase C is given by

$$J_{PIP2}=\frac{1}{1+\exp\left(\frac{MP_h-\Delta_c\phi}{S_{MP}}\right)}\times\frac{[PIP_2]^3}{(K_M^{PIP2})^3+[PIP_2]^3}\times L^{max}_{PIP2}\times RT\ln\left[\frac{[PIP_2][c^0]}{[IP_3][DG]}\times K'_{PIP2}\right]. \tag{A25}$$

$L^{max}_{PIP2}=4.0\times10^{-8}(\mu M/ms)\times(mol/J), K'_{PIP2}$ was set to $K'_{ATPc}=5.76\times10^5$, $MP_h=-56$ mV, $S_{MP}=1.0$ mV, $K_M^{PIP2}=1.0$ μM.

Flux through IP_3 phosphatase is given by

$$J_{IP3}=\frac{[IP_3]^3}{(K_M^{IP3})^3+[IP_3]^3}\times L^{max}_{IP3}\times RT\ln\left[\frac{[IP_3]}{[IP_2]}\frac{[c^0]}{[Pi]}\times K'_{IP3}\right]. \tag{A26}$$

$L^{max}_{IP3}=1.0\times10^{-8}(\mu M/ms)\times(mol/J), K'_{IP3}$ was set to $K'_{ATPc}=5.76\times10^5, K_M^{IP3}=1.0\times10^{-8}$.

The two next dephosphorylation steps of the cascade were contracted to one single step yielding

$$J_{IP2}=\frac{1}{1+\exp\left(\frac{[Ca_h^{2+}]_r^{ph}-[Ca^{2+}]_r}{[S_{caph}]_r}\right)}\times\frac{[IP_2]^3}{(K_M^{IP2})^3+[IP_2]^3}\times L^{max}_{IP2}\times RT\ln\left[\frac{[IP_2]}{[In]}\frac{[c^0]^2}{[Pi]^2}\times(K'_{IP2})^2\right]. \tag{A27}$$

$L^{max}_{IP2}=0.2\times10^{-8}(\mu M/ms)\times(mol/J)$, K'_{IP3} was set to K'_{ATPc}, $K_M^{IP2}=2.0$ μM, $[Ca_h^{2+}]_r^{phos}=200$ μM, $[Scaph]_r=20$ μM.

Resynthesis of PIP_2 from In and DAG starts from DAG phosphorylation by ATP and cytidine monophosphate activation to yield PI in the presence of In [cf. 45]. Two further phosphorylation steps are needed to get PIP_2. Thus five ATPs are used up to complete the cycle. The flux proceeds however at a rather low velocity, so that ATP consumption by the cycle is negligible. Five reaction steps are contracted to one single step yielding

$$J_{In}=\frac{[In]^2}{\left(K_M^{phA}\right)^2+[In]^2}\times L^{max}_{phA}\times RT\ln\left[\frac{[In]}{[PIP2]}\frac{[DG]}{[Pi]^2}\frac{[ATP]^5[c^0]}{[ADP]^5}\times K'_{phA}\right]. \tag{A28}$$

$L^{max}_{phA}=0.18\times10^{-8}(\mu M/ms)\times(mol/J),\quad K_M^{phA}=4.0$ μM, K'_{phA} was adjusted to 1.0.

Fluxes of the ER membrane

Flux through SERCA2 Ca^{2+} pumps is given by

$$J_{SR2}=\alpha_c\times\frac{1}{1+\exp\left(\frac{[Ca^{2+}]_r-[Ca_h^{2+}]_r^{SR2}}{[S_{SR2}]}\right)}\frac{[Ca^{2+}]_c^2}{(K_M^{SR2})^2+[Ca^{2+}]_c^2}\frac{[FBP]^2}{(K_M^{FBP})^2+[FBP]^2}\times G^{max}_{SR2}\times\left((\lambda_{SR3ca}+1)\times\frac{RT}{F}\ln\left(\frac{[Ca^{2+}]_c^2}{[Ca^{2+}]_r^2}\frac{[H^+]_r^4}{[H^+]_c^4}+\tilde{A}_{ATPc}\right)\right), \tag{A29}$$

$G^{max}_{SR2}=12$ pS, $[Ca_h^{2+}]_r^{SR2}=200$ μM, $[S_{SR2}]=20$ μM, $K_M^{SR2}=0.4$ μM, $K_M^{FBP}=1.0$ μM.

Flux through SERCA3 Ca^{2+} pumps is given by

$$J_{SR3} = \alpha_c \times \frac{1}{1+\exp\left(\frac{[Ca^{2+}]_r - [Ca_h^{2+}]_r^{SR3}}{[S_{SR3}]}\right)} \frac{[Ca^{2+}]_c^2}{(K_M^{SR3})^2 + [Ca^{2+}]_c^2} \times G_{SR3}^{max} \times \left((\lambda_{SR3ca}+1) \times \frac{RT}{F} \ln\left(\frac{[Ca^{2+}]_c^2}{[Ca^{2+}]_r^2}\frac{[H^+]_r^4}{[H^+]_c^4} + \tilde{A}_{ATPc}\right)\right). \tag{A30}$$

$$G_{SR3}^{max} = 15pS, \quad [Ca_h^{2+}]_r^{SR3} = 300\mu M, \quad [S_{SR3}] = 10\mu M, \quad K_M^{SR3} = 2.0\mu M.$$

Flux through Ca^{2+} release channel is given by

$$J_{Rel} = \frac{\alpha_c}{2} \times \frac{1}{1+\exp\left(\frac{[Ca_h^{2+}]_r^{Rel} - [Ca^{2+}]_r}{[S_{Rel}]}\right)} \frac{1}{1+\exp\left(\frac{[IP_{3h}]-[IP_3]}{[S_{IP3}]}\right)} \times G_{Rel}^{max} \times \frac{RT}{F} \ln\left[\frac{[Ca^{2+}]_r}{[Ca^{2+}]_c}\frac{[H^+]_c}{[H^+]_r} \times 1\right]. \tag{A31}$$

The factor "1" in the logarithmic argument is caused by a charge compensating ionic flux in series having zero driving force.

$$G_{Rel}^{max} = 100pS, \quad [Ca_h^{2+}]_r^{Rel} = 30\mu M, \quad [S_{Rel}] = 400\mu M, \quad [IP_{3h}] = 1.2\mu M, \quad [S_{IP3}] = 0.4\mu M.$$

Power output reactions

The flux through Na-K pump was changed to include now $[K^+]_c$ and $[Na^+]_c$ as variables. It is given by

$$J_{NaK} = \alpha_c \times \frac{[Na^+]_c^3}{(K_M^{NaK})^3 + [Na^+]_c^3} \frac{[K^+]_e^5}{(K_M^{Ke})^5 + [K^+]_e^5} \times G_{NaK}^{max} \times \left(-3\left(\frac{RT}{F}\ln\left(\frac{[Na^+]_e}{[Na^+]_c}\right) - \Delta_c\phi\right) + 2\left(\frac{RT}{F}\ln\left(\frac{[K^+]_e}{[K^+]_c}\right) - \Delta_c\phi\right) + \tilde{A}_{ATPc}\right). \tag{A32}$$

G_{NaK}^{max} = 15 pS, K_M^{NaK} = 10 mM, K_M^{Ke} = 2.0 mM. A voltage-dependent inactivation of the pump reaction as shown by Chapman [4] was not incorporated, because interference with $\Delta_c\phi$ during activation could not be adequately compensated.

The flux through the Ca^{2+} pump of the cell membrane is given by

$$J_{PMCA} = \alpha_c \cdot \frac{[Ca^{2+}]_c^2}{(K_M^{CP})^2 + [Ca^{2+}]_c^2} \cdot G_{CP}^{max} \times \left(\frac{RT}{F}\ln\left(\frac{[Ca^{2+}]_c}{[Ca^{2+}]_e}\frac{[H^+]_e^2}{[H^+]_c^2}\right) + \tilde{A}_{ATPc}\right), \tag{A33}$$

$$[H^+]_e = 10^{-1.4} \quad \text{and} \quad [Ca^{2+}]_e = 1.2 \times 10^3 \mu M, G_{max}^{CP} = 16.0pS, \quad K_M^{CP} = 0.4\mu M.$$

The flux through the reactions of insulin secretion is given by

$$J_{Exo} = \alpha_c \times \frac{1}{1+\exp\left(\frac{\{DG_h\}-\{DG\}}{\{S_{DG}\}}\right)} \frac{[Ca^{2+}]_c^2}{(K_M^{Exo})^2 + [Ca^{2+}]_c^2} \times G_{Exo}^{max} \times \left(\frac{RT}{F}\ln(Load_{Exo}) + \tilde{A}_{ATPc}\right). \tag{A34}$$

G_{Exo}^{max} = 8.2 pS, $\{DG_h\}$ = 3.0 μM, $\{S_{DG}\}$ = 1.0 μM, K_M^{Exo} = 0.4 μM, $Load_{Exo}$ is set constant to 3.2×10^{-3}. Curly braces indicate membrane concentrations in mol/dm^2.

The flux through reactions of protein biosynthesis is given by

$$J_{Pbs} = \frac{1}{1+\exp\left(\frac{[IP_2]-[IP_{2h}]}{[S_{IP2}]}\right)} \times L_{Pbs}^{max} \times [RT\ln(Load_{Pbs}) + A_{ATPc}]. \tag{A35}$$

$$L_{Pbs}^{max} = 92 \times 10^{-8}(\mu M/ms) \times (mol/J), \quad [IP_{2h}] = 4.0\mu M, \quad [S_{Pbs}] = 0.8\mu M, \quad Load_{Pbs} = 5 \times 10^{-6}.$$

All parallel fluxes of total ADP production (ATP consumption) are given by

$$J_P = J_{NaK} + J_{MPCA} + J_{SR2} + J_{SR3} + J_{Exo} + J_{Pbs} + 5J_{In}. \tag{A36}$$

ADP utilisation (ATP production) is given by

$$J_U = (\alpha_c/\alpha_m)J_{AE} + 2\ (J_{Ga} - J_{GK}), \tag{A37}$$

J_{GK} and J_{Ga} are given below (B1 and B4, respectively).

Additional currents of the cell membrane

A depolarising, non-selective cation current is included now, which is activated by $[IP_2]$ in present simulations. The respective channel is known to be permeable to Na^+ and K^+ under physiological conditions. The sum of Na^+ and K^+ currents through these channels is given by

$$\begin{aligned} I_{CRAN} &= G_{Na}^{CRA}A_{Na} + G_K^{CRA}A_K = G_{Na}^{CRA} \times \left(A_{Na} + \frac{G_K^{CRA}}{G_{Na}^{CRA}}A_K\right), \\ &= G_{Na}^{CRA} \times \left(\frac{RT}{F}\ln\left(\frac{[Na^+]_e}{[Na^+]_c}\right) - z_{Na}\,\Delta_c\phi + Q_G^{CRA} \times \left[\frac{RT}{F}\ln\left(\frac{[K^+]_e}{[K^+]_c}\right) - z_K\Delta_c\phi\right]\right), \quad \text{or for} \quad z_{Na} = z_K = 1, \end{aligned} \tag{A38a}$$

$$I_{CRAN} = G_{Na}^{CRA}\left(1 + Q_G^{CRA}\right) \times \left(\frac{RT}{F\left(1 + Q_G^{CRA}\right)}\ln\left(\frac{[Na^+]_e}{[Na^+]_c}\ \left(\frac{[K^+]_e}{[K^+]_c}\right)^{Q_G^{CRA}}\right) - \Delta_c\phi\right). \tag{A38b}$$

The equilibrium potential of this current is given by

$$E_{CRAN} = \frac{RT}{F\left(1 + Q_G^{CRA}\right)}\ln\left(\frac{[Na^+]_e}{[Na^+]_c}\ \left(\frac{[K^+]_e}{[K^+]_c}\right)^{Q_G^{CRA}}\right). \tag{A38c}$$

The value of E_{CRAN} is about −15 mV. Inserting this value into Eq. (A34a) for $I_{CRAN}=0$ yields $Q_G^{CRA}=1.2432$. The full current is given then by

$$I_{CRAN} = \frac{1}{1 + \exp\left(\frac{[IP_{2h}^{CRA}] - [IP_2]}{[S_{IP2}^{CRA}]}\right)} \times \left(1 + Q_G^{CRA}\right)G_{CRAN}^{max} \times \left(\frac{RT}{F}\ln\left(\frac{[Na^+]_e}{[Na^+]_c}\right) - \Delta_c\phi + Q_G^{CRA} \times \left(\frac{RT}{F}\ln\left(\frac{[K^+]_e}{[K^+]_c}\right) - \Delta_c\phi\right)\right). \tag{A38d}$$

$G_{CRAN}^{ax}=2.0$ pS, $[IP_{2h}^{CRA}]=4.0$ μM, $[S_{IP2}^{CRA}]=0.4$ μM. The first factor on the right hand side of Eq. (A34c) causes activation by $[IP_2]$. I_{CRAN}^{Na} and I_{CRAN}^{K} denote the Na^+ fraction and K^+ fraction of the current, respectively. These fractional currents are given by total I_{CRAN}, whose A_K or A_{Na}, respectively, was set to zero.

A Na^+ leak current had to be added to the sum of cell membrane currents to match in part the hyperpolarising current of the Na-K pump. This current is given by

$$I_{NaL} = G_{NaL}^{max} \times \left(\frac{RT}{F}\ln\left(\frac{[Na^+]_e}{[Na^+]_c}\right) - \Delta_c\phi\right). \tag{A39}$$

$G_{NaL}^{max} = 14.5$pS.

pH and pMg dependent binding polynomials are now included into the conductance of the K_{ATP} channel, to show how pH and/or pMg changes of the cytosol might influence the opening characteristics of this channel. The current through this channel is given by

$$I_{Katp} = \frac{0.08\left(1 + \frac{1}{P_{MgADP-}}\frac{2[ADP]_c}{K_{dd}}\right) + 0.89\left(\frac{1}{P_{MgADP-}}\frac{2[ADP]_c}{K_{dd}}\right)^2}{\left(1 + \frac{1}{P_{MgADP-}}\frac{[ADP]_c}{K_{dd}}\right)^2 \times \left(1 + \frac{1}{P_{ADP3-}}\frac{[ADP]}{K_{td}} + \frac{1}{P_{ATP4-}}\frac{[ADP]}{K_{tt}}\right) - \left(\frac{1}{P_{MgADP-}}\frac{[ADP]_c}{K_{dd}}\right)^2} \times G_{Katp}^{max} \times \left(\frac{RT}{F}\ln\left(\frac{[K^+]_e}{[K^+]_c}\right) - \Delta_c\phi\right). \tag{A40}$$

G_{Katp}^{max} of 4000 pS was not changed, K_{tt} was changed from 22 to 43.9 μM, K_{td} and K_{dd} remained unchanged at values of 57 and 31 μM, respectively.

B. Taken over equations from reference [17]

The flux through GK plus PFK is given by

$$J_{GK} = \frac{[Glu]^2}{(K_M^{GK})^2+[Glu]^2}\ \frac{[ADP]_c^2}{(K_M^{PF})^2+[ADP]_c^2}\ L_{GK}^{max} \times RT\ln\left(\frac{[Glu]}{[FBP]}\ \frac{[ATP]_c^2}{[ADP]_c^2} \times K'_{GK}\right), \tag{B1}$$

$[ATP]_c=[S]_c-[ADP]_c$, $[S]_c$, was set to 4.0×10^3 μM, $K'_{GK}=8.022\times10^7$, L_{GK}^{max} was set to 12×10^{-8} (μM/ms)×(mol/J), K_M^{GK} and K_M^{PF} were adjusted to 5.5×10^3 and 250 μM, respectively.

The flux through aldolase is given by

$$J_{Al} = \frac{[FBP]}{K_M^{Al}+[FBP]} L_{Al}^{max} \times RT\ln\left(\frac{[FBP]\ [c^0]}{[GAP]\ [DHAP]} \times K'_{Al}\right), \tag{B2}$$

GAP=glyceraldehyde-3-phosphate, DHAP=dihydroxyacetone phosphate, $K'_{A1}=9.2329\times10^{-5}$, $K_M^{A1}=0.2$ μM, $L_{A1}^{max}=150\times10^{-8}$ (μM/ms)×(mol/J).

The flux through triose phosphate isomerise is given by

$$J_{Ti} = \frac{[DHAP]}{K_M^{Ti}+[DHAP]} \cdot L_{Ti}^{max} \times RT\ln\left(\frac{[DHAP]}{[GAP]} \times K'_{Ti}\right), \tag{B3}$$

$K'_{Ti}=0.0455$, $L_{Ti}^{max}=600\times10^{-8}$ (μM/ms)×(mol/J), $K_M^{Ti}=4$ μM.

The flux through glyceraldehyde-3-phosphate dehydrogenase is given by

$$J_{Ga} = \frac{[GAP]}{K_M^{Ga}+[GAP]}\ L_{Ga}^{max} \times RT\ln\left(\frac{[GAP]}{[Pyr]_c} \times \frac{[ADP]_c^2\ [Pi]_c}{[ATP]_c^2\ [c^0]} \times \frac{[NAD_{ox}]_c}{[NAD_{red}]_c} \times K'_{Ga}\right), \tag{B4}$$

$K'_{Ga}=4.8393\times10^5$, Pyr_c=cytosolic pyruvate, $[NAD_{ox}]_c=[NAD_t]_c-[NAD_{red}]_c$, $[NAD_t]_c$ was set to 500 μM.

$$L_{max}^{Ga} = 80\times10^{-8}(\mu M/ms)\times(mol/J), \quad L_m^{Ga} = 2.0\ \mu M.$$

The flux through proton/pyruvate cotransport is given by

$$J_{Pym} = \alpha_m\ \frac{[Pyr]_c^3}{(K_M^{PYm})^3+[Pyr]_c^3}\ G_{Pym}^{max} \times \frac{RT}{F}\ln\left(\frac{[Pyr]_c}{[Pyr]_m} \times \frac{[H^+]_c}{[H^+]_m}\right), \tag{B5}$$

$G_{Pym}^{max} = 190pS, \quad K_M^{Pym} = 50\ \mu M.$

The flux through glycerophosphate shuttle is given by

$$J_{GS} = \alpha_m\ \frac{[DHAP]^3}{(K_M^{DS})^3+[DHAP]^3}\ \frac{[Ca^{2+}]_c^2}{(K_M^{CS})^2+[Ca^{2+}]_c^2}\frac{[NAD_{red}]_c^3}{(K_M^{FS})^3+[NAD_{red}]_c^3} \times G_{GS}^{max}\ \frac{RT}{F}\ln\left(\frac{[NAD_{red}]_c}{[NAD_{ox}]_c} \times \frac{[FAD_{ox}]_m}{[FAD_{red}]_m} \times K'_{GS}\right), \tag{B6}$$

$K'_{GS} = 3.5844\times10^{10}, \quad G_{GS}^{max} = 38pS, \quad K_M^{DS} = 30, \quad K_M^{CS} = 1.2, \quad \text{and} \quad K_M^{FS} = 0.5\ \mu M.$

The flux through malate–aspartate shuttle is given by

$$J_{MS} = \alpha_m \frac{[NAD_{red}]_c^3}{(K_M^{NS})^3+[NAD_{red}]_c^3} G_{MS}^{max} \times \left(\frac{RT}{F}\ln\left(\frac{[NAD_{red}]_c}{[NAD_{ox}]_c} \times \frac{[NAD_{ox}]_m}{[NAD_{red}]_m}\right) - \Delta_m\tilde{\mu}_H\right), \tag{B7a}$$

$$\Delta_m\tilde{\mu}_H = \frac{RT}{F}\cdot\ln\left(\frac{[H^+]_m}{[H^+]_c}\right) + \Delta_m\phi, \tag{B7b}$$

$G_{MS}^{max}=4.94$ pS, $K_M^{NS}=0.5$ μM.

The flux through the redox span NAD_{red}/O_2 is given by

$$J_{NA} = \frac{\alpha_m}{\nu_n} \frac{[NAD_{red}]_m^3}{(K_M^{NA})^3 + [NAD_{red}]_m^3} G_{NA}^{max} \times \left(\frac{RT}{F} \ln\left(\frac{[NAD_{red}]_m}{[NAD_{ox}]_m} \times \frac{[O_2]^{0.5}}{[c^0]^{0.5}} \times K'_{NA} \right) + \nu_n \Delta_m \tilde{\mu}_H(mV) \right), \tag{B8}$$

$K'_{NA} = 1.6858 \times 10^{38}$, $[O_2]$ was set constant to 35 μM, $G_{NA}^{max} = 1140$ pS, $K_M^{NA} = 6.0$ μM, $\nu_n = 10$.

The flux through the redox span $FAD_{red}/O_2$is given by

$$J_{FA} = \frac{\alpha_m}{\nu_f} \frac{[FAD_{red}]_m^3}{(K_M^{FA})^3 + [FAD_{red}]_m^3} G_{FA}^{max} \times \left(\frac{RT}{F} \ln\left(\frac{[FAD_{red}]_m}{[FAD_{ox}]_m} \times \frac{[O_2]^{0.5}}{[c^0]^{0.5}} \times K'_{FA} \right) + \nu_f \Delta_m \tilde{\mu}_H(mV) \right), \tag{B9}$$

$K'_{FA} = 3.6229 \times 10^{26}$, $G_{FA}^{max} = 1710$ pS, $K_M^{FA} = 0.5$ μM, $\nu_f = 6$.

The flux of O_2 consumption is given by

$$J_{O2} = \frac{\alpha_c}{2\,\alpha_m} (J_{NA} + J_{FA}). \tag{B10}$$

The flux through Ca^{2+} uniporter is given by

$$J_{CU} = \frac{\alpha}{2} \frac{[Ca^{2+}]_c^3}{(K_M^{CU})^3 + [Ca^{2+}]_c^3} G_{CU}^{max} \times \left(\frac{RT}{F} \ln\left(\frac{[Ca^{2+}]_c}{[Ca^{2+}]_m} \right) - 2\,\Delta_m\phi \right), \tag{B11}$$

$G_{max}^{CU} = 38$ pS, $K_M^{CU} = 1.0$ μM.

The flux through the H/Ca exchange reaction is given by

$$J_{HCE} = \alpha \frac{[Ca^{2+}]_m^3}{(K_M^{HC})^3 + [Ca^{2+}]_m^3} G_{HC}^{max} \times \frac{RT}{F} \ln\left(\frac{[Ca^{2+}]_m}{[Ca^{2+}]_c} \times \frac{[H^+]_c^2}{[H^+]_m^2} \right), \tag{B12}$$

$G_{HC}^{max} = 38$ pS, $K_M^{HC} = 1.0$ μM.

The proton leak flux through the inner mitochondrial membrane is given by

$$J_{PL} = \alpha_m G_{PL} \times \left(\frac{RT}{F} \ln\left(\frac{[H^+]_c}{[H^+]_m} \right) - \Delta_m\phi \right), \tag{B13}$$

$G_{PL} = 12$ pS.

The flux through the Na/Ca exchange reaction is given by

$$J_{NCE} = \alpha_c \frac{[Ca^{2+}]_c}{(K_M^{NC}) + [Ca^{2+}]_c} G_{NC}^{max} \times \left(\frac{RT}{F} \ln\left(\frac{[Ca^{2+}]_c}{[Ca^{2+}]_e} \right) + 3\,\frac{RT}{F} \ln\left(\frac{[Na^+]_c}{[Na^+]_e} \right) - \Delta_c\phi \right). \tag{B14}$$

$[Na^+]_e = 143 \times 10^3$ and $[Ca^{2+}]_e = 1.2 \times 10^3$ μM, $G_{max}^{NC} = 6.0$ pS, $K_M^{NC} = 0.8$ μM.

The current through Ca_V channels is given by

$$I_{Cav} = \frac{1}{1 + e^{\left(\frac{V_m - \Delta_c\phi}{s_m}\right)}} \cdot \frac{1}{1 + e^{-\left(\frac{V_h - \Delta_c\phi}{s_h}\right)}} G_{Ca}^{max} \times \left(\frac{RT}{F} \ln\left(\frac{[Ca^{2+}]_e}{[Ca^{2+}]_c} \right) - \Delta_c\phi \right), \tag{B15}$$

$V_m = 4.0$ mV, $s_m = 14.2$ mV, $V_h = -2.0$, $s_h = 10$ mV, and $G_{Ca}^{max} = 600$ pS.

The outward delayed rectifier K^+ current is given by

$$I_{\mathrm{Kre}} = n \cdot G_{\mathrm{Kre}}^{\max} \times \left(\frac{RT}{F} \ln\left(\frac{[\mathrm{K}^+]_{\mathrm{e}}}{[\mathrm{K}^+]_{\mathrm{c}}} \right) - \Delta_{\mathrm{c}}\phi \right). \tag{B16}$$

$$\frac{dn}{dt} = \frac{\left(\frac{1}{1+e^{\left(\frac{V_{\mathrm{n}} - \Delta_{\mathrm{c}}\phi}{s_{\mathrm{n}}} \right)}} \right) - n}{\tau_{\mathrm{n}}}. \tag{B17}$$

$V_{\mathrm{n}} = -15$ mV, $s_{\mathrm{n}} = 5.6$ mV, $G_{\mathrm{Kre}}^{\max} = 2500$ pS, and $\tau_{\mathrm{n}} = 20$ ms.

Differential equations

$$\frac{d(\Delta_{\mathrm{m}}\phi)}{dt} = \frac{1}{Cm_{\mathrm{m}} \cdot \alpha_{\mathrm{m}}} \times \left(\frac{1}{\nu_{\mathrm{s}}} J_{\mathrm{SY}} + J_{\mathrm{AE}} + 2J_{\mathrm{CU}} + J_{\mathrm{MS}} + J_{\mathrm{PL}} - \nu_{\mathrm{n}} J_{\mathrm{NA}} - \nu_{\mathrm{f}} J_{\mathrm{FA}} \right).$$

$$\frac{d[\mathrm{H}^+]_{\mathrm{m}}}{dt} = \frac{1}{1 + \kappa_1^{\mathrm{BU}} + \kappa_2^{\mathrm{BU}}} \times \left(\frac{1}{\nu_{\mathrm{s}}} J_{\mathrm{SY}} + J_{\mathrm{Pi}} + J_{\mathrm{PL}} + J_{\mathrm{MS}} + 2J_{\mathrm{HC}} + J_{\mathrm{CAm}} - \nu_{\mathrm{n}} J_{\mathrm{NA}} - \nu_{\mathrm{f}} J_{\mathrm{FA}} \right).$$

$$\frac{d[\mathrm{NAD_{red}}]_{\mathrm{m}}}{dt} = J_{\mathrm{PDH}} + 3J_{\mathrm{CAC}} + J_{\mathrm{MS}} - J_{\mathrm{NA}}.$$

$$\frac{d[\mathrm{FAD_{red}}]_{\mathrm{m}}}{dt} = J_{\mathrm{CAC}} + J_{\mathrm{GS}} - J_{\mathrm{FA}}.$$

$$\frac{d[\mathrm{ADP}]_{\mathrm{m}}}{dt} = J_{\mathrm{AE}} - J_{\mathrm{CAC}} - J_{\mathrm{SY}}.$$

$$\frac{d[\mathrm{Ca}^{2+}]_{\mathrm{m}}}{dt} = \frac{1}{1 + \kappa_{\mathrm{Cam}}} \times (J_{\mathrm{CU}} - J_{\mathrm{HC}}).$$

$$\frac{d[\mathrm{Pi}]_{\mathrm{m}}}{dt} = J_{\mathrm{Pi}} - J_{\mathrm{SY}} - J_{\mathrm{CAC}}.$$

$$\frac{d[\mathrm{ADP}]_{\mathrm{c}}}{dt} = J_{\mathrm{Exo}} + J_{\mathrm{Pbs}} + 2J_{\mathrm{GK}} + J_{\mathrm{NaK}} + J_{\mathrm{PMCA}} - J_{\mathrm{AE}} - 2J_{\mathrm{Ga}}.$$

$$\frac{d[\mathrm{Pi}]_{\mathrm{c}}}{dt} = J_{\mathrm{Exo}} + J_{\mathrm{Pbs}} + J_{\mathrm{NaK}} + J_{\mathrm{PMCA}} - J_{\mathrm{Pi}} - J_{\mathrm{Ga}}.$$

$$\frac{d[\mathrm{Pyr}]_{\mathrm{m}}}{dt} = J_{\mathrm{Pym}} - J_{\mathrm{PDH}}.$$

$$\frac{d[\mathrm{Pyr}]_{\mathrm{c}}}{dt} = J_{\mathrm{Ga}} - J_{\mathrm{Pym}}.$$

$$\frac{d[\mathrm{NAD_{red}}]_{\mathrm{c}}}{dt} = J_{\mathrm{Ga}} - J_{\mathrm{MS}} - J_{\mathrm{GS}}.$$

$$\frac{d[\mathrm{FBP}]}{dt} = J_{\mathrm{GK}} - J_{\mathrm{Al}}.$$

$$\frac{d[\mathrm{GAP}]}{dt} = J_{\mathrm{Al}} + J_{\mathrm{Ti}} - J_{\mathrm{Ga}}.$$

$$\frac{d[\mathrm{DHAP}]}{dt} = J_{\mathrm{Al}} - J_{\mathrm{Ti}}.$$

$$\frac{d(\Delta_c\phi)}{dt} = \frac{1}{Cm_c} \times \left(I_{\mathrm{Cav}} + I_{\mathrm{Kre}} + I_{\mathrm{Katp}} + I_{\mathrm{CRAN}} + I_{\mathrm{NaL}} + \frac{1}{\alpha_c} J_{\mathrm{NCE}} - \frac{1}{\alpha_c} J_{\mathrm{NaK}} \right).$$

$$\frac{d\left[\mathrm{Ca}^{2+}\right]_c}{dt} = \frac{1}{1+\kappa_{\mathrm{Cac}}} \times \left(\frac{\alpha_c}{2} I_{\mathrm{Ca}} + J_{\mathrm{HC}} + J_{\mathrm{Rel}} - J_{\mathrm{PMCA}} - J_{\mathrm{CU}} - J_{\mathrm{NCE}} - J_{\mathrm{SR2}} - J_{\mathrm{SR3}} \right).$$

$$\frac{dn}{dt} = \frac{\left(\frac{1}{1+\exp\left(\frac{V_n - \Delta_c\phi}{s_n}\right)} \right) - n}{\tau_n}.$$

Additional new variables

$$\frac{d\left[\mathrm{Ca}^{2+}\right]_r}{dt} = \frac{1}{1+\kappa_{\mathrm{Car}}} \times (2J_{\mathrm{SR2}} + 2J_{\mathrm{SR3}} - J_{\mathrm{Rel}}).$$

$$\frac{d[\mathrm{H}^+]_c}{dt} = \frac{1}{1+\kappa_1^{\mathrm{BU}} + \kappa_2^{\mathrm{BU}}} \times (J_{\mathrm{CA}} + 4J_{\mathrm{SR2}} + 4J_{\mathrm{SR3}} + 2J_{\mathrm{PMCA}} - J_{\mathrm{NHE}} - J_{\mathrm{Rel}}).$$

$$\frac{d[\mathrm{Na}^+]_c}{\mathrm{d}t} = J_{\mathrm{NHE}} + 3J_{\mathrm{NCE}} + J_{\mathrm{NaL}} + \alpha_c I_{\mathrm{CRAN}}^{\mathrm{Na}} - 3J_{\mathrm{NaK}}.$$

$$\frac{d[\mathrm{K}^+]_c}{dt} = 2J_{\mathrm{NaK}} + \alpha_c I_{\mathrm{Katp}} + \alpha_c I_{\mathrm{Kre}} + \alpha_c I_{\mathrm{CRAN}}^{\mathrm{K}}.$$

$$\frac{d[\mathrm{CO}_2]_m}{dt} = J_{\mathrm{PDH}} + 2J_{\mathrm{CAC}} - J_{\mathrm{CO2m}} - J_{\mathrm{CAm}}.$$

$$\frac{d[\mathrm{CO}_2]_c}{dt} = J_{\mathrm{CO2m}} - J_{\mathrm{CAc}} - J_{\mathrm{CO2c}}.$$

$$\frac{d\left[\mathrm{HCO}_3^-\right]_m}{dt} = J_{\mathrm{CAm}}.$$

$$\frac{d\left[\mathrm{HCO}_3^-\right]_c}{dt} = J_{\mathrm{CAc}} - J_{\mathrm{AnE}}.$$

$$\frac{d[\mathrm{IP}_3]}{dt} = J_{\mathrm{PIP2}} - J_{\mathrm{PI3}}.$$

$$\frac{d[\mathrm{IP}_2]}{dt} = J_{\mathrm{IP3}} - J_{\mathrm{IP2}}.$$

$$\frac{d[\mathrm{In}]}{dt} = J_{\mathrm{IP2}} - J_{\mathrm{In}}.$$

$$\frac{d\{\mathrm{PIP}_2\}}{dt} = J_{\mathrm{In}} - J_{\mathrm{PIP2}}.$$

$$\frac{d\{\mathrm{DG}\}}{dt} = J_{\mathrm{PIP2}} - J_{\mathrm{In}}.$$

$$\frac{d[\mathrm{AcCoA_{red}}]_m}{dt} = J_{PDH} - J_{CAC}.$$

$1+\kappa_{Cam}=200$, $1+\kappa_{Cac}=100$, $1+\kappa_{Car}=50$.

The following fluxes of my recent article [cf. 17] were renamed: J_{CP}, J_{NC}, J_{HCE}, and J_{SP} are now designated as J_{PMCA}, J_{NCE}, J_{HCE}, and J_{NaK}, respectively.

Appendix B. Supplementary data

Supplementary data associated with this article can be found, in the online version, at doi:10.1016/j.bpc.2008.02.001.

References

[1] R.A. Alberty, Thermodynamics of biochemical reactions, Wiley-Interscience, New York, 2003.

[2] W.F. Hopkins, S. Fatherazi, B. Peter-Riesch, B.E. Corkey, D.L. Cook, Two sites for adenine-nucleotide regulation of ATP-sensitive potassium channels in mouse pancreatic beta-cells and HIT cells, J. Membr. Biol. 129 (1992) 287–295.

[3] J.C. Skou, The identification of the sodium pump, Biosci. Rep. 24 (2004) 436–451.

[4] J.B. Chapman, Thermodynamics and kinetics of electrogenic pumps, Soc. Gen. Physiol. Ser. 38 (1984) 17–32.

[5] W. Chen, R. Dando, Electrical activation of Na/K pumps can increase ionic concentration gradient and membrane resting potential, J. Membr. Biol. 214 (2006) 147–155.

[6] M.W. Roe, M.E. Lancaster, R.J. Mertz, J.F. Worley 3rd, I.D. Dukes, Voltage-dependent intracellular calcium release from mouse islets stimulated by glucose, J. Biol. Chem. 268 (1993) 9953–9956.

[7] J.F. Worley 3rd, M.S. McIntyre, B. Spencer, R.J. Mertz, M.W. Roe, I.D. Dukes, Endoplasmic reticulum calcium store regulates membrane potential in mouse islet beta-cells, J. Biol. Chem. 269 (1994) 14359–14362.

[8] J.F. Worley 3rd, M.S. McIntyre, B. Spencer, I.D. Dukes, Depletion of intracellular Ca2+ stores activates a maitotoxin-sensitive nonselective cationic current in beta-cells, J. Biol. Chem. 269 (1994) 32055–32058.

[9] D. Mears, N.F. Sheppard Jr., I. Atwater, E. Rojas, R. Bertram, A. Sherman, Evidence that calcium release-activated current mediates the biphasic electrical activity of mouse pancreatic beta-cells, J. Membr. Biol. 155 (1997) 47–59.

[10] M.W. Roe, R.J. Mertz, M.E. Lancaster, J.F. Worley 3rd, I.D. Dukes, Thapsigargin inhibits the glucose-induced decrease of intracellular Ca2+ in mouse islets of Langerhans, Am. J. Physiol. 266 (1994) E852–E862.

[11] R. Bertram, L. Satin, M. Zhang, P. Smolen, A. Sherman, Calcium and glycolysis mediate multiple bursting modes in pancreatic islets, Biophys. J. 87 (2004) 3074–3087.

[12] R. Bertram, L.S. Satin, M.G. Pedersen, D.S. Luciani, A. Sherman, Interaction of glycolysis and mitochondrial respiration in metabolic oscillations of pancreatic islets, Biophys. J. 92 (2007) 1544–1555.

[13] R. Bertram, A. Sherman, L.S. Satin, Metabolic and electrical oscillations: partners in controlling pulsatile insulin secretion, Am. J. Physiol., Endocrinol Metab. 293 (2007) E890–E900.

[14] M.C. Beauvois, C. Merezak, J.C. Jonas, M.A. Ravier, J.C. Henquin, P. Gilon, Glucose-induced mixed $[Ca^{2+}]_c$ oscillations in mouse beta-cells are controlled by the membrane potential and the SERCA3 Ca^{2+}-ATPase of the endoplasmic reticulum, Am. J. Physiol., Cell Physiol. 290 (2006) C1503–C1511.

[15] J.-C. Henquin, H.P. Meissner, W. Schmeer, Cyclic variations of glucose-induced electrical activity in pancreatic B cells, Pflügers Arch. 393 (1982) 322–327.

[16] D.L. Cook, Isolated islets of Langerhans have slow oscillations of electrical activity, Metabolism 32 (1983) 681–685.

[17] F. Diederichs, Mathematical simulation of membrane processes and metabolic fluxes of the pancreatic beta-cell, Bull. Math. Biol. 68 (2006) 1779–1818.

[18] M.J. Berridge, Unlocking the secrets of cell signalling, Annu. Rev. Physiol. 67 (2005) 1–21.

[19] D.F.S. Rolfe, G.C. Brown, Cellular energy utilisation and molecular origin of standard metabolic rate in mammals, Physiol. Rev. 77 (1997) 731–758.

[20] S. Göpel, T. Kanno, S. Barg, J. Galvanovskis, P. Rorsman, Voltage-gated and resting membrane currents recorded from B-cells in intact mouse pancreatic islets, J. Physiol. 521 (1999) 717–728.

[21] R.D. Vaughan-Jones, K.W. Spitzer, P. Swietach, Spatial aspects of intracellular pH regulation in heart muscle, Prog. Biophys. Mol. Biol. 90 (2006) 207–224.

[22] F. Thévenod, Ion channels in secretory granules of the pancreas and their role in exocytosis and release of secretory proteins, Am. J. Physiol., Cell Physiol. 283 (2002) C651–C672.

[23] P. Stiernet, Y. Guiot, P. Gilon, J.C. Henquin, Glucose acutely decreases pH of secretory granules in mouse pancreatic islets. Mechanisms and influence on insulin secretion, J. Biol. Chem. 281 (2006) 22142–22151.

[24] N.M. Doliba, S.L. Wehrli, M.Z. Vatamaniuk, W. Qin, C.W. Buettger, H.W. Collins, F.M. Matschinsky, Metabolic and ionic coupling factors in amino acid-stimulated insulin release in pancreatic beta-HC9 cells, Am. J. Physiol., Endocrinol Metab. 292 (2007) E1507–E1519.

[25] J.-C. Henquin, A.E. Lambert, Extracellular bicarbonate ions and insulin secretion, Biochim. Biophys. Acta 381 (1975) 437–442.

[26] P.B. Carroll, M.X. Li, E. Rojas, I. Atwater, The ATP-sensitive potassium channel in pancreatic B-cells is inhibited in physiological bicarbonate buffer, FEBS Lett. 234 (1988) 208–212.

[27] G.G. MacGregor, K. Dong, C.G. Vanoye, L. Tang, G. Giebisch, S.C. Hebert, Nucleotides and phospholipids compete for binding to the C terminus of K_{ATP} channels, Proc. Natl. Acad. Sci. U. S. A. 99 (2002) 2726–2731.

[28] D.E. Atkinson, Cellular energy metabolism and its regulation, Academic press, New York, 1977, p. 218.

[29] F. Buttgereit, M.D. Brand, A hierarchy of ATP-consuming processes in mammalian cells, Biochem. J. 312 (1995) 163–167.

[30] W.F. Boron, E.L. Boulpaep, Medical Physiology, Elsevier Inc., 2005.

[31] P. Gilon, J.-C. Henquin, Influence of membrane potential changes on cytoplasmic Ca^{2+} concentration in an electrically excitable cell, the insulin-secreting pancreatic B-cell, J. Biol. Chem. 267 (1992) 20713–20720.

[32] P. Gilon, A. Arredouani, P. Gailly, J. Gromada, J.C. Henquin, Uptake and release of Ca^{2+} by the endoplasmic reticulum contribute to the oscillations of the cytosolic Ca^{2+} concentration triggered by Ca^{2+} influx in the electrically excitable pancreatic B-cell, J. Biol. Chem. 274 (1999) 20197–20205.

[33] A. Arredouani, Y. Guiot, J.-C. Jonas, L.H. Liu, M. Nenquin, J.A. Pertusa, J. Rahier, J.-F. Rolland, G.E. Shull, M. Stevens, F. Wuytack, J.-C. Henquin, P. Gilon, SERCA3 ablation does not impair insulin secretion but suggests distinct roles of different sarcoendoplasmic reticulum Ca^{2+} pumps for Ca^{2+} homeostasis in pancreatic beta-cells, Diabetes (United States) 51 (2002) 3245–3253.

[34] A. Arredouani, J.-C. Henquin, P. Gilon, Contribution of the endoplasmic reticulum to the glucose-induced $[Ca^{2+}]_c$ response in mouse pancreatic islets, Am. J. Physiol., Endocrinol Metab. 282 (2002) E982–E991.

[35] G. Magnus, Keizer, Model of β-cell Ca^{2+} handling and electrical activity. I. Cytoplasmic variables, Am. J. Physiol. 274 (1998) C1158–C1173.

[36] L.E. Fridlyand, N. Tamarina, L.H. Philipson, Modeling of Ca2+ flux in pancreatic beta-cells: role of the plasma membrane and intracellular stores, Am. J. Physiol., Endocrinol Metab. 285 (2003) E138–E154.

[37] J. Lytton, M. Westlin, S.E. Burk, G.E. Shull, D.H. MacLennan, Functional comparisons between isoforms of the sarcoplasmic or endoplasmic reticulum family of calcium pumps, J. Biol. Chem. 267 (1992) 14483–14489.

[38] S.R. Caplan, A. Essig, Bioenergetics and linear nonequilibrium thermodynamics the steady state, Harvard University Press, London, England, 1983.

[39] S.R. Caplan, A. Essig, Bioenergetics and linear nonequilibrium thermodynamics the steady state, Harvard University Press, London, England, 1983.

[40] D. Pietrobon, S.R. Caplan, Use of nonequilibrium thermodynamics in the analysis of transport: general flow–force relationships and the linear domain, Methods Enzymol 171 (1989) 397–444.
[41] T.F. Weiss, Cellular biophysics, volume 1: Transport, MIT Press, Cambridge, Massachusetts, 1996.
[42] M. Marhl, S. Schuster, M. Brumen, Mitochondria as an important factor in the maintenance of constant amplitudes of cytosolic calcium oscillations, Biophys. Chem. 71 (1998) 125–132.
[43] R.T. Kennedy, L.M. Kauri, G.M. Dahlgren, S.K. Jung, Metabolic oscillations in beta-cells, Diabetes 51 (Suppl 1) (2002) 152–161.
[44] E. Neher, The use of Fura-2 for estimating Ca buffers and Ca fluxes, Neuropharmacology 34 (1995) 1423–1442.
[45] D. Voet, J.G. Voet, Biochemistry, John Wiley & Sons, Inc., New York, 1995.